https://doi.org/10.5194/egusphere-2025-418
Preprint. Discussion started: 24 February 2025

Likely breaks in cloud cover retrievals complicate attribution of the trend in the Earth Energy Imbalance

Jippe Hoogeveen[1], Jan Fokke Meirink[2], and Frank Selten[2]
[1]Utrecht University
[2]KNMI
Correspondence: Jippe Hoogeveen (jippehoogeveen1@gmail.com)

Abstract. There is a broad scientific consensus that the earth is warming due to anthropogenic emissions of greenhouse gases (GHG). Increasing GHGs decrease the outgoing longwave radiation (OLR) at the top of the atmosphere (TOA). Since climate change is driven by the Earth Energy Imbalance (EEI), it is crucial to have accurate estimates of the TOA radiative fluxes and identify the factors that drive the observed trend in EEI. In this research, we examined satellite-measured TOA radiative fluxes. In accordance with other studies we found a substantial increase in the absorbed solar radiation (ASR) and a smaller increase in OLR since 2000, which indicates that increased ASR played an important role in recent global warming. We derived a statistical model that quantifies the contribution of different factors to the observed trends in ASR and OLR. We found that the assessment of the contribution of trends in clouds is complicated due to inhomogeneities in retrieved clear-sky fluxes and the underlying cloud datasets. A formal break detection algorithm strongly suggests the existence of breaks in especially low cloud cover. The cloud effect on ASR is therefore relatively hard to estimate, but it is likely a major cause of the increase in ASR. OLR can be more accurately reproduced with cloud cover, temperature and water vapour changes, but the expected decrease due to GHG was not found. We conclude that the inhomogeneities detected in this study warrant more study as they impact the attribution of the trend in EEI.

1 Introduction

The radiative fluxes at the top of the atmosphere (TOA) determine the energy balance of the earth-atmosphere system. The Earth Energy Imbalance (EEI) is given by the Absorbed Solar Radiation (ASR) minus the Outgoing Longwave Radiation (OLR). A positive EEI implies an accumulation of energy in the Earth system. The sun emits shortwave (SW) radiation, which enters the earth's atmosphere, partly reflects back to space and the remainder is absorbed in the atmosphere and by the earth's surface. Clouds, aerosols, water vapour and atmospheric gases like ozone influence the reflection and absorption in the atmosphere. The optical properties of the ocean and land surfaces determine the reflection and absorption at the surface. Whether or not snow or ice is present has a large impact on the reflection. The earth's surface emits longwave (LW) radiation, which is partly absorbed and re-emitted by atmospheric constituents. It is important to understand and quantify the influence of all of these factors on OLR and ASR and thus on the radiative balance of the earth-atmosphere system as this balance controls the temperature of the earth.

https://doi.org/10.5194/egusphere-2025-418
Preprint. Discussion started: 24 February 2025

In particular the impact of clouds on OLR and ASR is important. The net radiative effect of a cloud depends on its height and other properties like optical depth (Chen et al., 2000). Low clouds tend to be thicker and thus reflect more SW radiation, while due to their warm tops, the net absorption of LW radiation is small. On the other hand, high clouds are generally thinner and reflect a smaller portion of the SW radiation, while their cold tops lead to a strong net absorption of LW radiation. As such, low clouds tend to have a strong cooling effect and high clouds tend to have a slight warming effect. Globally averaged the reflection of SW radiation by clouds exceeds their absorption of LW. Thus clouds cool the earth.

Monitoring of TOA radiative fluxes has been enabled by satellite observations since around 1980. The most comprehensive measurements of TOA fluxes as well as cloud coverage have been compiled by the Clouds and the Earth's Radiant Energy System (CERES) program, starting in March 2000 (Loeb et al., 2018; Kato et al., 2018; Loeb et al., 2024). These measurements show that since 2000, both ASR and OLR have increased, with the net effect leading to an increase in EEI (Loeb et al., 2021). Using radiative transfer calculations, the trends in ASR and OLR have been attributed to different factors. Loeb et al. (2021) found that (for the period 2002-2020) the ASR trend is mainly due to a decrease in reflection of radiation by clouds ($\approx 65\%$) and to a smaller extent to a decrease in surface albedo ($\approx 30\%$). For OLR they found that changes in clouds and temperature have contributed to the upward trend, with the temperature change having the strongest effect. Increases in water vapour and well-mixed greenhouse gases have counteracted the upward trend. The estimated reduction in OLR due to the increase in well-mixed greenhouse gases (0.2 Wm^{-2} per decade) is half the Effective Radiative Forcing of the well-mixed greenhouse gasses as reported in (Dentener et al., 2021) in Annex III for the period 2000 to 2020. We do not know why these two estimates of the radiative effect of well-mixed greenhouse gases between 2000 and 2020 differ so much, but it might be due to different assumptions made in separating the effects of clouds and greenhouse gases on the OLR. Similar reductions in OLR as reported by Loeb et al. (2021) due to an increase in greenhouse gas concentrations were obtained in other studies, e.g., Kramer et al. (2021). Whitburn et al. (2021) used measurements of the flux at different wavelengths from the Infrared Atmospheric Sounding Interferometer (IASI) and found significant decreases in the spectral absorbing regions of greenhouse gases in the tropics. De Longueville et al. (2021) found a clear fingerprint of multiple trace gases using the IASI measurements, both for wildfires in Australia at the start of 2020 and for the difference between 2017 and 2008 in the clear-sky fluxes for different spectral lines. Teixeira et al. (2024) use similar measurements from the Atmospheric Infrared Sounder (AIRS) to detect the radiative effect of greenhouse gases: they create a reference from random clear-sky samples from 2003 and compare later measurements from 2003-2012 with the best fitting reference from 2003 based on temperature and water vapour. The difference should be due to the increase in greenhouse gases and they are able to find their spectral fingerprints. The reduction in OLR due to an increase in greenhouse gases is thus well-established, both from radiative transfer calculations as well as from direct measurements with satellites, but various estimates of the magnitude of the trend on a global scale differ.

On the other hand, the radiative response due to cloud changes is less well understood. It is expected that clouds act as a positive feedback to both OLR and ASR when temperature increases, but the magnitude of this feedback is still not entirely certain (Masson-Delmotte et al., 2023). For example Goessling et al. (2025) found that a decrease in low cloud cover might explain the unexpectedly high recent global temperature peek in 2023 and 2024. Also Olonscheck and Rugenstein (2024) found that the latest generations of climate models underestimate the trend in TOA net flux. This indicates that attribution of

https://doi.org/10.5194/egusphere-2025-418
Preprint. Discussion started: 24 February 2025

the radiative flux changes (mainly estimating the cloud effect) and determining whether the effects are natural variation or feedbacks is very important.

In this paper, we attempted to attribute trends in TOA radiative fluxes to cloud cover changes, temperature and water vapour changes and remaining factors (such as greenhouse gases for OLR and surface albedo changes and aerosols for ASR). However these estimates require stable measurements over long time periods as inhomogeneities in the measurements can severely impact trend estimates. Stable data records are difficult to obtain for radiative fluxes and even more so for cloud properties. Therefore, in this paper, we examine several available satellite datasets of clouds and TOA radiation, and check them specifically for possible inhomogeneities. In addition to all-sky fluxes, also clear-sky fluxes, derived with a regression technique, are analysed. Effects of possible inhomogeneities on trend estimates are quantified.

The organization of this report is as follows. In Sect. 2 the data records are described and we outline how we use these records in this study. Section 3 describes the analysis we conducted. In Sect. 4, the datasets are compared and their homogeneity is assessed. In Sect. 5, we discuss the results of our investigations. Finally in Sect. 6, the conclusions are presented.

2 Datasets

In this section, we describe the different datasets we used. Most datasets do not directly provide ASR, but rather provide the reflected solar radiation. We estimate the ASR from these measurements by assuming that the incoming solar radiation is constant. This is of course not entirely true, but since the variations in incoming solar radiation are small, we neglect these variations in this study.

2.1 CERES

CERES Energy Balanced and Filled (EBAF) 4.2 provides all-sky and clear-sky observations of the OLR and reflected solar radiation (Loeb et al., 2018). These are derived from two satellites, namely Terra from March 2000 onward and Aqua from July 2002 onward. In April 2022 the new satellite NOAA-20 continued the ASR and OLR measurements, but that period is not examined here. The data is provided at a resolution of 1 degree.

For the clear-sky fluxes, CERES uses output of the Moderate Resolution Imaging Spectroradiometer (MODIS) instrument alongside the cloud cover retrieved by a collection of geostationary satellites. For cloudy pixels, radiation calculations based on MODIS cloud information are used to determine a clear sky flux.

The CERES (Single Scanner Footprint) SSF (version SSF1deg) product includes cloud cover retrieved from the polar satellites Terra, Aqua, S-NPP and NOAA-20 (Doelling et al., 2013). For this paper, we focused on Terra and Aqua, since the other two satellites do not cover a long enough period. We averaged the measurements from Terra and Aqua. In the CERES SSF data, cloud cover is reported at four heights (Low, Mid-Low, Mid-High and High) for day-time only (solar zenith less than 90°) and for day and night. The low level clouds lie below 700 hPa, the mid-low level clouds lie between 500 hPa and 700 hPa, the mid-high level clouds between 300 hPa and 500 hPa and the high level clouds lie above 300 hPa.

https://doi.org/10.5194/egusphere-2025-418
Preprint. Discussion started: 24 February 2025

The cloud data from CERES have been retrieved from the same MODIS instruments for the entire period. However, different retrieval algorithms based on MODIS measurements were used: MODIS Collection 5 (C5) up until February 2016 and MODIS Collection 6.1 (C61) from March 2016 onward (CERES, 2024).

2.2 ISCCP-H

The International Satellite Cloud Climatology Project (ISCCP) dataset is determined from a combination of many different geostationary and polar satellites (Young et al., 2018); (Rossow et al., 2022). We used TOA radiative fluxes and cloud cover from the ISCCP-H (HGM/HGH) product, beginning in July 1983 and ending in June 2017, at a 1 degree resolution. The cloud coverage is provided on 3 levels, namely Low, Middle and High. The low level clouds lie below 680 hPa, the middle level clouds between 440 hPa and 680 hPa and the high level clouds lie above 440 hPa.

2.3 CLARA-A3

The third edition of the CLoud, Albedo and RAdiation dataset, AVHRR-based (CLARA-A3) is based on measurements from the Advanced Very High Resolution Radiometer (AVHRR) aboard polar satellites from the NOAA and Metop series (Karlsson et al., 2023). The measurements start in January 1979 and continue until present, and are provided at a resolution of 0.25 degrees. We used TOA radiative fluxes and cloud cover, provided at the same levels (Low, Middle and High) as ISCCP-H. The sampling with AVHRR instruments has not been constant over time. In particular, before 2002, only two satellites were available at a given time, while from 2002 onward always at least three satellites have been active. In addition, there have been changes in the shortwave infrared channels: most of the time channel 3B (around 3.7 μm) has been used. However, on all mid-morning satellites as well as on NOAA-16 from October 2000 until April 2003 channel 3A (around 1.6 μm) has been active during daytime.

2.4 Cloud_cci

The Cloud_cci dataset is another dataset containing both cloud properties and TOA radiative fluxes derived from AVHRR measurements (Stengel et al., 2020). The dataset starts in January 1982 and continues until present at a 0.5-degree resolution. In this study, we only examined the TOA radiative fluxes.

2.5 HIRS

The NOAA High resolution Infrared Radiation Sounder (HIRS) dataset provides OLR, derived using the HIRS instruments aboard the satellites from NOAA (Lee et al., 2007). The data record starts in January 1979 and continues until present at a 2.5-degree resolution. There have been 3 types of HIRS instrument versions, namely HIRS 2, HIRS 2I and HIRS 3. HIRS 2 was mainly used before 1990, HIRS 2I from 1990 to 2000 and HIRS 3 from 2000 onward. As the HIRS instruments were mounted on the same satellites as the AVHRR instruments, the same changes in sampling over time apply as mentioned in Sect. 2.3.

https://doi.org/10.5194/egusphere-2025-418
Preprint. Discussion started: 24 February 2025

2.6 ERA5

ERA5 is a global reanalysis dataset (Hersbach et al., 2020). The dataset starts in 1950 and continues until present at a 0.25-degree resolution. From ERA5 we used the TOA radiative fluxes.

2.7 UAH temperature data

The UAH dataset provides the temperature at different levels of the atmosphere, namely lower troposphere (LT), middle troposphere (MT), tropopause (TP) and lower stratosphere (LS) (Spencer R.W., 2017). It uses the Microwave Sounding Unit (MSU) and Advanced Microwave Sounding Unit - A (AMSU-A) satellite instruments to measure the radiation emitted by oxygen molecules, from which the temperature is derived. The temperature retrievals are provided at a 2.5-degree resolution, starting in January 1979 and continuing until present. The instruments are mounted on the NOAA and Metop satellite series with AMSU-A replacing MSU around 2000.

3 Methods

In this section we elaborate on two methodological aspects. Sect. 3.1 describes how the effect of variations in clouds and temperature on the time series of all-sky fluxes are estimated. In Sect. 3.2 the detection of break points is discussed.

3.1 Estimating the effect of variations in clouds and temperature on all-sky fluxes

In order to attribute trends in radiative fluxes, we statistically estimate the effect of cloud cover variations on both the ASR and OLR fluxes and additionally the effect of temperature and water vapour variations on the OLR flux. In so far these effects are linear, subtracting these estimates from the all-sky fluxes should eliminate most of the fast and longer term changes in the radiative fluxes related to these variables and present mainly the greenhouse gas forcing (GHG) for OLR and the surface albedo (SA) and aerosol (AER) changes for ASR. We used the temperature data of UAH as an approximation for both the temperature and the amount of water vapour, since the amount of water vapour covaries approximately linearly with temperature (Allan et al., 2022).

There are two ways in which we estimated the influence of clouds. The first uses the clear sky data from CERES and we estimated the cloud radiative effect by subtracting the clear-sky flux from CERES from the all-sky flux. The second uses cloud cover observations from CLARA-A3, ISCCP and CERES SSF. We apply a linear regression technique for estimating the effect of clouds on ASR and OLR. A linear regression of OLR on temperature is applied to estimate the combined effect of temperature and water vapour on OLR. The regressions are based on monthly mean, global averaged values. Global averages of temperature and clouds are regionally weighted. Specifically, in order to estimate the effect of cloud cover on all-sky ASR we calculated the global mean cloud cover based on weighted gridded monthly mean cloud cover using the mean clear-sky ASR times the grid cell area as weights. This is appropriate since the effect of clouds on ASR is proportional to the flux in the absence of clouds. For the correction of OLR, cloud cover was weighted by the monthly mean clear-sky OLR times the grid cell area. This is appropriate since the absorbed LW flux by clouds is proportional to the OLR in the absence of clouds. Temperature was weighted with the monthly mean OLR to the power of $\frac{3}{4}$. This is appropriate since OLR is proportional to the temperature to the power of 4:

$$Q = C \cdot T^4$$

, where Q is the OLR, T the temperature and C a constant. In the regressions, only small variations around the absolute temperature T occur, so in good approximation, we can write $T = T_0 + dT$ with T_0 the average baseline temperature and dT the small variations. Now we find that

$$Q = C \cdot T^4 = C \cdot (T_0 + dT)^4 = C \cdot T_0^4 + 4CT_0^3 dT + O(dT^2)$$

Neglecting the higher order terms, we find that we should weigh with T_0^3 or $Q^{\frac{3}{4}}$.

CERES clear-sky fluxes do not need to be corrected for clouds, so only regressions against temperature were made for OLR, and no regressions were performed for ASR. The cloud radiative effect is then added as an estimate of the influence of clouds and temperature on OLR and clouds on ASR.

For CLARA-A3 and ISCCP we took the low, middle and high cloud cover as explanatory variables rather than total cloud coverage, to account for the different radiative effect of clouds at different heights. For CERES SSF we used a further separation of low, mid-low, mid-high and high cloud cover into day-plus-night for estimating the cloud effect on OLR, and daytime-only for ASR.

We did not attempt to attribute the remaining residuals as was done in Loeb et al. (2021), because remaining influences as changes in the composition of the atmosphere are harder to estimate using linear regression on monthly variations as atmospheric composition variations on a monthly timescale are relatively small as compared to the long-term trend. However, we did add a trend as explanatory variable in all regressions in order to account for trend-like influences by the statistical model. When we show residuals in the paper, we did not remove the trend-like influence, only the estimated effect of clouds and temperature. As noted before, we did not distinguish between the effect of temperature and water vapour, because these are highly correlated and thus cannot be separated using linear regression. In the results section, we also present the distribution of the total OLR or ASR trend over the different factors with 95%-confidence intervals. Here blue denotes cooling (so positive OLR and negative ASR trend) and red denotes warming (so negative OLR and positive ASR trend).

3.2 Testing for break points

We used the BEAST (a Bayesian Estimator of Abrupt change, Seasonal change and Trend) software package (Zhao et al., 2019) to make quantitative estimates of the presence and magnitude of break points. This algorithm divides the dataset into parts with the same trend and seasonal cycle, split by break points. In our case, the seasonal cycle was neglected as all datasets were deseasonalized. BEAST provides estimates of the probabilities of a break point at a certain moment in time. These estimates do not take additional knowledge into account such as a change in measurement. We first tested this method on computer generated datasets to test these probabilities.

https://doi.org/10.5194/egusphere-2025-418
Preprint. Discussion started: 24 February 2025

For our test dataset, we drew 240 (which might correspond to 20 years worth of monthly values) independent standard normally distributed numbers. BEAST should detect no break point in these timeseries. Next a break point was introduced between data point 120 and 121 by adding a constant c to data points 121 to 240. We expect BEAST to detect a break point between data point 120 and 121 in this case. We tested $c = 0.1, 0.2, 0.5, 1$ and $c = 2$. We did 100 runs for each value of c and record the probabilities. With $c = 0$ (so no break point), we took the highest probability for a break point found by BEAST in the entire dataset, as this illustrates the probability of BEAST reporting a break point when there is none. For the other values of c, we picked the highest probability for a break point detected anywhere between data points 100 and 140. In table 1, the average probabilities found in these experiments over 100 runs are shown.

c	Probability
0	0.1703 [0.1513, 0.2009]
0.1	0.1473 [0.0931, 0.2094]
0.2	0.1489 [0, 0.275]
0.5	0.3007 [0.1082, 0.8955]
1	0.722 [0.3173, 0.9886]
2	0.9937 [0.9274, 1]

Table 1. Average probabilities found by BEAST over 100 runs with different jump sizes c. The mean of the highest probabilities per run is reported, for $c = 0$ over the entire interval and for $c > 0$ over the interval $[100, 140]$. The confidence intervals are calculated by taking the 2.5-th and 97.5-th percentile of these highest probabilities.

Table 1 first of all shows that BEAST will find maximum probabilities just below 0.2 if the time series is completely homogeneous, so a probability of above 0.2 generally indicates that there really is a break point, although small break points might still get a probability below 0.2 according to BEAST. However when this break point is small, it is not very likely to be detected. Only from $c = 0.5$ the probability really increases although there is a very large confidence interval for both $c = 0.5$ and $c = 1$: this indicates that sometimes, BEAST is relatively sure, although it might even miss the break point. For $c = 0.5$, BEAST found in 41 out of 100 runs that the probability was smaller than 0.2 so not larger than in a random dataset with no inhomogeneities. This indicates that we should be careful when testing for small break points with BEAST as they have significant probability not to be picked up. On the other hand for $c = 1$, BEAST found probabilities above 0.2 for all runs so these larger break points, larger than one standard deviation, are likely to be picked up. For $c = 2$, two times the standard deviation, we see that BEAST is generally very sure and only found probabilities below 0.95 in 4 out of 100 runs.

For $c > 0$, we also recorded where BEAST placed the break point (we only counted it if it is between 100 and 140). We ignored the cases in which BEAST detected a break point outside this range. The probability of this happening is small: it did not happen for $c = 0.1$, $c = 1$ and $c = 2$ and it happened in only 6 runs for $c = 0.2$ and in 1 run for $c = 0.5$ out of 100 runs. In table 2 the averages with confidence intervals are tabulated. The actual value should be 121 as the break point is located between 120 and 121.

https://doi.org/10.5194/egusphere-2025-418
Preprint. Discussion started: 24 February 2025

c	Time Index Inhomogeneity
0.1	119.19 $[100, 140]$
0.2	118.07 $[100, 139]$
0.5	118.68 $[101, 138]$
1	119.62 $[102.53, 129.95]$
2	120.85 $[118.53, 124]$

Table 2. The average time index at which BEAST locates the most probable break point between 100 and 140. The confidence intervals are calculated by taking the 2.5-th and 97.5-th percentile.

Table 2 shows that even for $c = 1$, the uncertainty in the timing of the break point is quite large, which means that BEAST may locate the break point up to a year earlier or later. Only for $c = 2$ BEAST is quite certain about the timing of the break. These test results help to interpret the application of BEAST to real datasets in the remainder of this paper.

In our experiments, BEAST is used on the residuals after correcting for cloud cover (and temperature for OLR). We use BEAST on these residuals instead of the uncorrected data, because we expect the residuals to have less natural variations, such that the inhomogeneities will show up more clearly.

4 Comparison between TOA radiation datasets

In this section we compare the different TOA radiation datasets, both for OLR and ASR.

Figure 1 shows OLR anomalies from CERES, HIRS, CLARA-A3, ERA5, Cloud_cci and ISCCP. After 2000, the data series agree relatively well: ISCCP and, to a lesser extent, Cloud_cci deviate most from the other four. Before 2000 the data series diverge substantially. This is also true for HIRS, CLARA-A3 and ERA5, which agree relatively well after 2000. CLARA-A3 and especially HIRS indicate that the OLR increased over the entire period whereas ERA5 shows little change or even a small decrease. The CERES dataset only starts in March 2000, so it can unfortunately not be used to assess these differences, and it is hard to judge which data series best represents the true OLR before 2000.

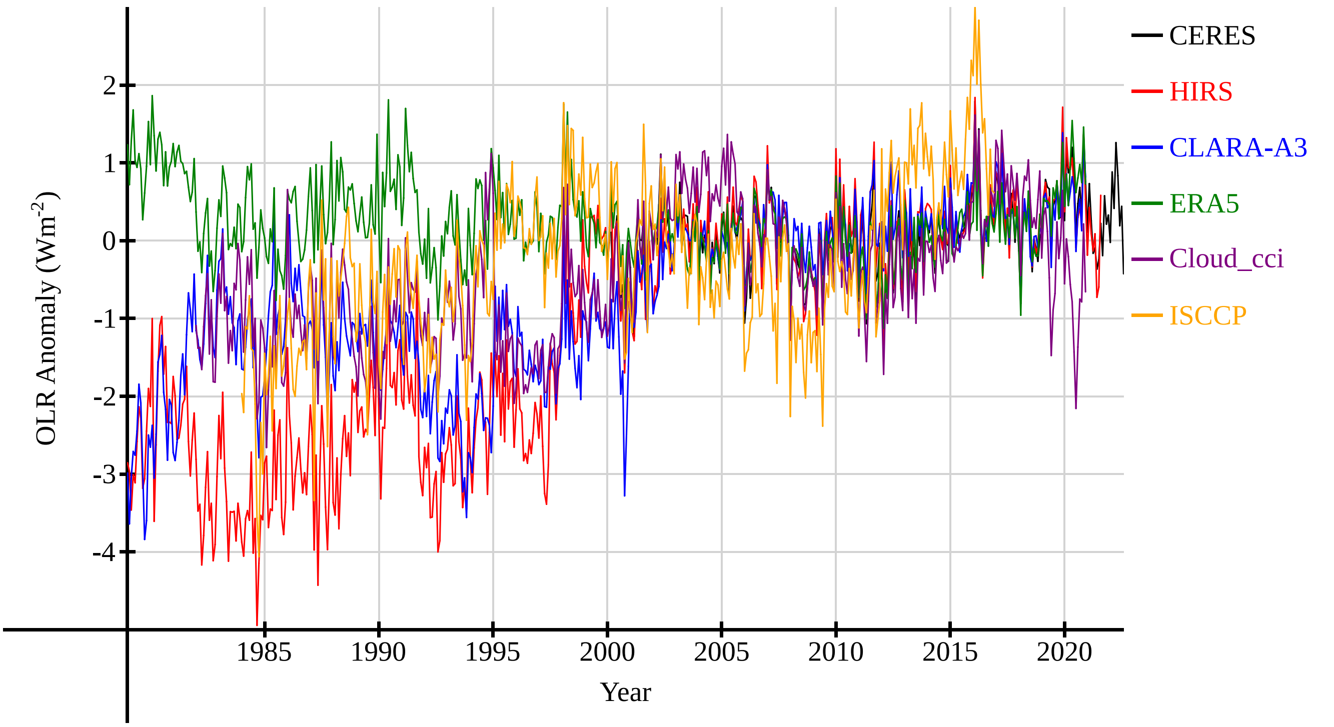

Figure 1. Comparison of global mean OLR from different datasets. Anomalies with respect to the overlap period March 2000 - December 2016 are shown.

Figure 2 repeats Fig. 1 for the period from 2000 onward with a reduced scale so it is easier to compare the data series during the period in which they agree most. ISCCP and Cloud_cci differ clearly from the other records. In addition, CLARA-A3 appears to be too low before 2003. Since CERES provides in principle the most accurate measurements of OLR, we will use that further on, and focus on the period after 2000. Given that especially CERES and HIRS agree so well, we assume that all-sky OLR is reliably measured by CERES.

https://doi.org/10.5194/egusphere-2025-418
Preprint. Discussion started: 24 February 2025

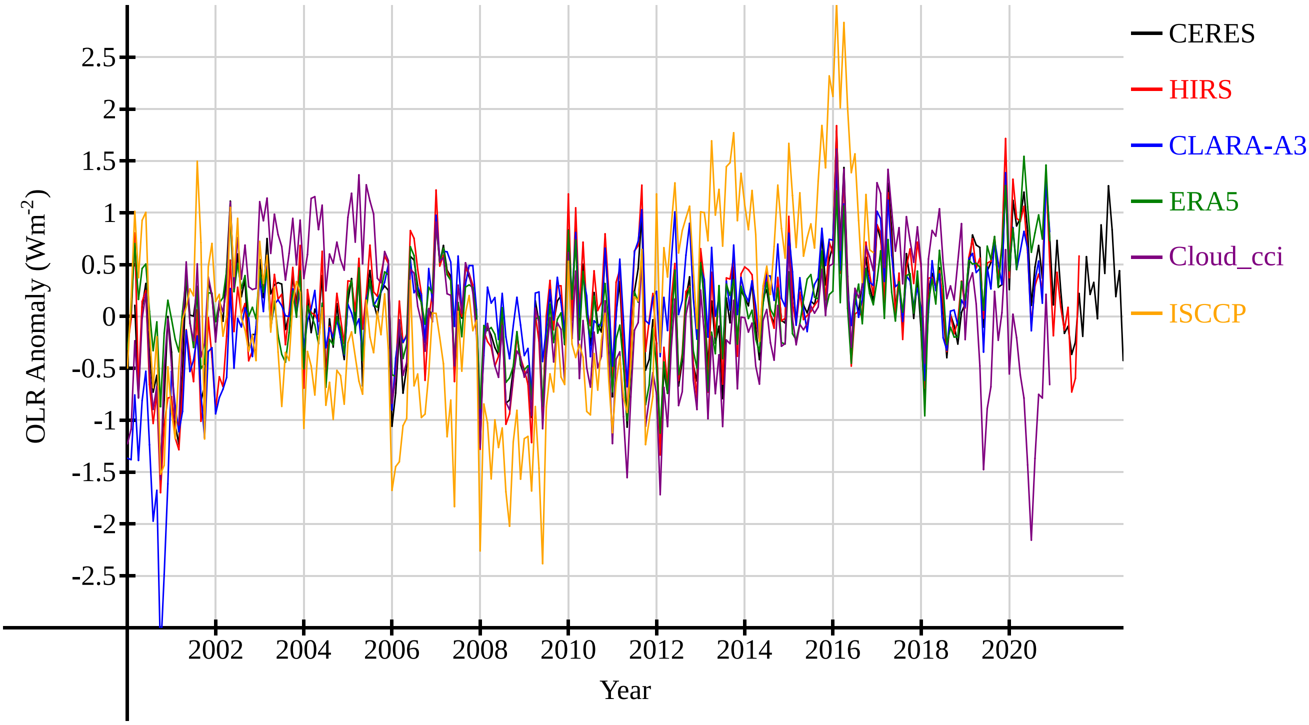

Figure 2. As Fig. 1 but for the period after 2000.

In Fig. 3, TOA ASR from CERES, CLARA-A3, ERA5, Cloud_cci and ISCCP are compared. Again some disagreement is seen before 2000, although less than for the OLR. This disagreement is most notable from 1995 until 2000. Around 1992, all data records show a dip, caused by scattering by aerosols injected into the stratosphere by the Pinatubo volcanic eruption. However, the data records do not agree on the magnitude of the dip. Before the Pinatubo eruption, the agreement is reasonable, although not as good as after 2000. After 2000, Cloud_cci seems to differ especially near the end of the record.

https://doi.org/10.5194/egusphere-2025-418
Preprint. Discussion started: 24 February 2025

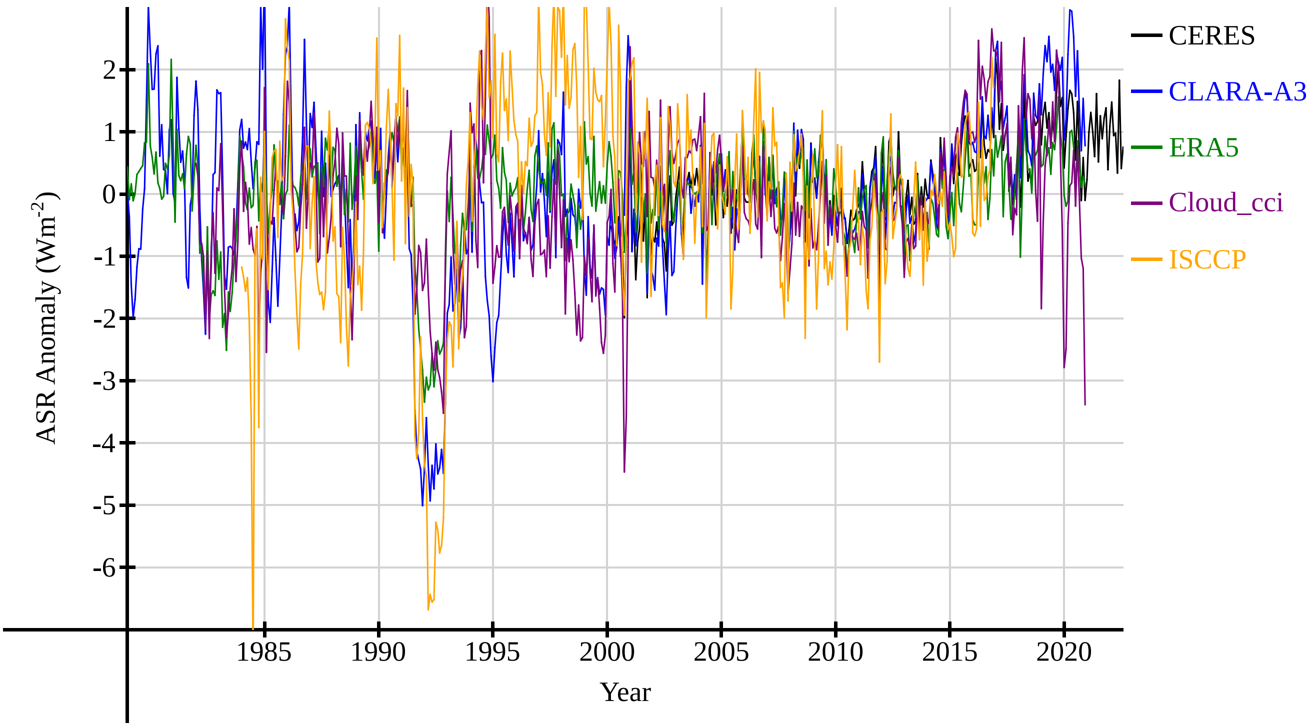

Figure 3. Comparison of global mean ASR from different datasets. Anomalies with respect to the overlap period March 2000 - December 2016 are shown.

A zoom-in of the ASR after 2000 with a smaller scale is shown in Fig. 4. It can be seen that ISCCP varies more than CERES, CLARA-A3 and ERA5. CLARA-A3 ASR seem to be too high at the end of the period. There is a bit more variance in ASR than in OLR between the different data series, but still the data series agree rather well. As mentioned before, the focus in the remainder of this study will be on the period after 2000. Again, since the ASR measurements are relatively comparable from 2000 onward, we assume that the all-sky ASR is measured reliable by CERES, although we are a bit less sure than with OLR.

https://doi.org/10.5194/egusphere-2025-418
Preprint. Discussion started: 24 February 2025

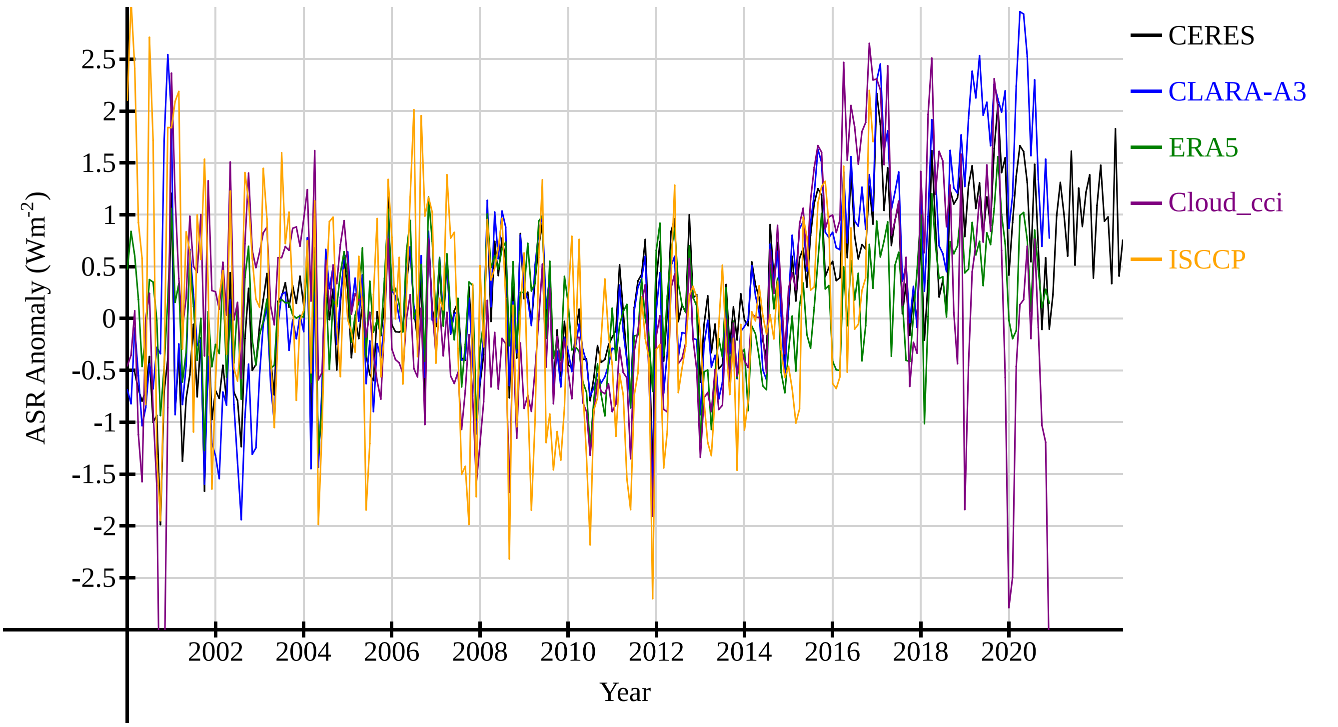

Figure 4. As Fig. 3 but for the period after 2000.

5 Results

In this section we show the results of the regression model that we use to relate the radiative flux changes of the CERES data to changes in clouds and temperature. The temperature and clouds related changes are subtracted and a formal break detection analysis is performed on the residuals. Likely breaks present in the timeseries are discussed. First, the CERES clear-sky data is used to calculate the cloud effect. Subsequently, ISCCP, CLARA-A3, and CERES SSF cloud data are used to estimate the cloud effect.

5.1 Regression with clear-sky data from CERES

Monthly all-sky OLR is modeled as the sum of the CERES clear-sky OLR that co-varies with temperature and the effects of clouds on OLR estimated by subtracting the all-sky minus clear-sky OLR from CERES. Modeled all-sky OLR is compared with the observed OLR in Fig. 5a. The observed and modeled monthly time series correlate rather well with $R = 0.7$ and the model tracks the fluctuations in OLR relatively well, especially on interannual scales. When taking a 12-month moving average, the correlation increases to $R = 0.75$. Figure 5b illustrates how the OLR trend is distributed over the different drivers. Mainly cloud changes contribute to the increase in OLR, whereas the increase in temperature and water vapour contributes slightly. Other drivers (mainly increasing GHG) partially counteract the increase in OLR. Figure 5c shows the residuals with a linear

https://doi.org/10.5194/egusphere-2025-418
Preprint. Discussion started: 24 February 2025

trend determined over the full time period. The trend is -0.27 ± 0.06 $\mathrm{Wm^{-2}}$ per decade. Potential break points are visible around January 2008 and March 2016. BEAST finds break points from December 2007 to January 2008 with probability 0.36 and from May to June 2016 with probability 0.4. Based on the tests in Section 3.2, these probabilities are higher than expected in a completely homogeneous setting, suggesting that there are indeed break points. In earlier CERES versions, a break in January 2008 could be explained by a switch between GEOS 4 and GEOS 5.2.1 model simulations used as input (Loeb et al., 2018). However, in CERES 4.2 this switch is not present anymore, and therefore we do not have an explanation for that break that is likely present. From February to March 2016, MODIS changed from version 5 to version 6.1. This seems to be the most likely reason for a possible break point in 2016 and we thus assume the break point was in March 2016. BEAST also detects a break point in 2004, but Fig. 5c suggests that this is a year with lower values rather than a real break. We also do not have a clear reason why there should be a break there, so we assume that it is just noise.

The total trends over the periods March 2000 until December 2007, January 2008 until February 2016 and March 2016 until December 2021 are -0.05 ± 0.29 $\mathrm{Wm^{-2}}$ per decade, 0.18 ± 0.26 $\mathrm{Wm^{-2}}$ per decade, and -0.36 ± 0.43 $\mathrm{Wm^{-2}}$ per decade, respectively (Fig. 5d). The first period does not really show a trend and the other trends are not significant. Thus, the significant negative trend over the full period disappears if trends are calculated separately for the periods between the potential breaks.

https://doi.org/10.5194/egusphere-2025-418
Preprint. Discussion started: 24 February 2025

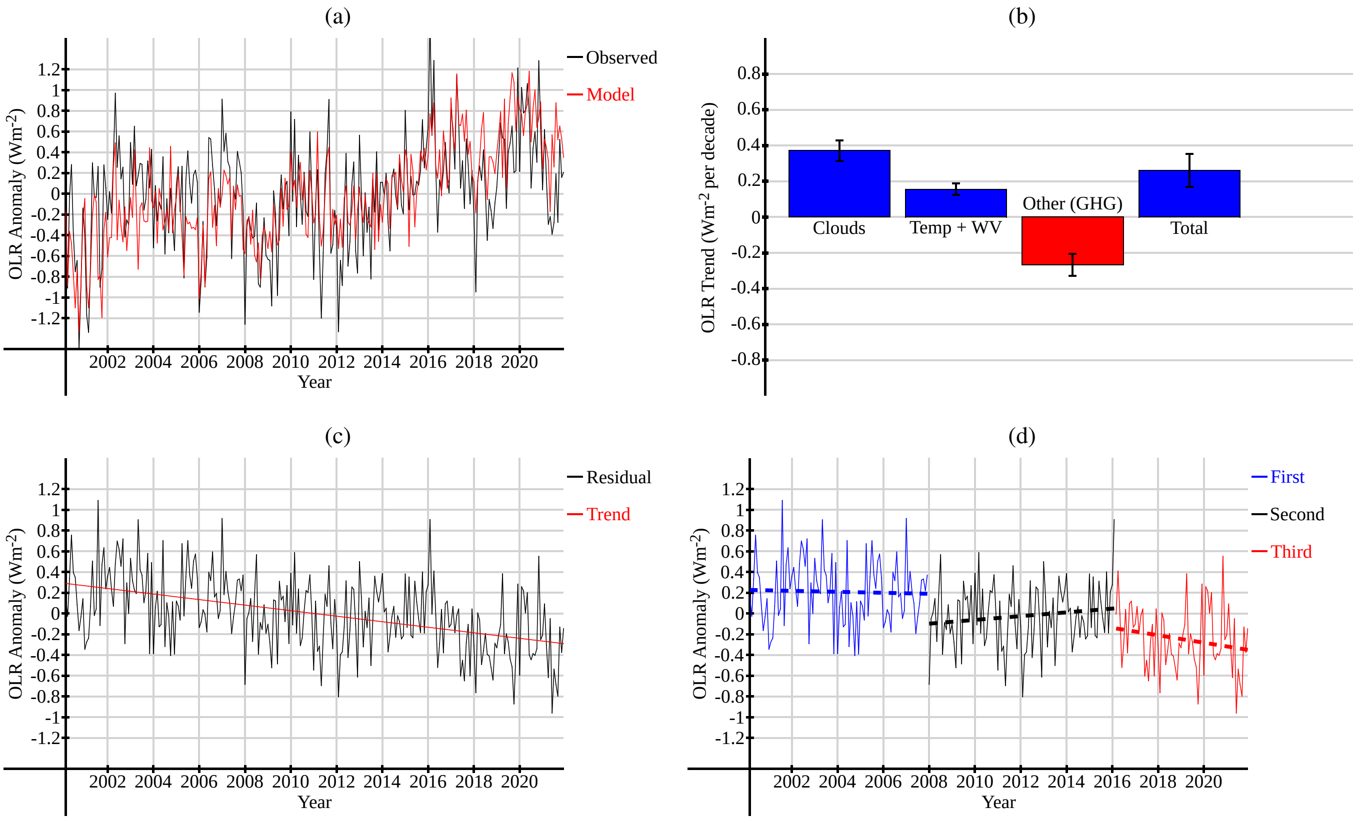

Figure 5. Explaining OLR using the clear-sky data of CERES to fix the cloud effect from March 2000 to December 2021: (a) comparison between the observed OLR and the regression model; (b) an attribution of the trend in OLR to trends in drivers; (c) residuals with linear trend; (d) residuals and trends calculated for the three periods separated by the possible break points in January 2008 and March 2016.

Figure 6a shows the results when the CERES all-sky minus clear-sky is used as cloud effect on ASR from March 2000 to December 2021. The cloud effect according to the CERES Clear-Sky data aligns again rather well with ASR with $R = 0.83$. When taking the 12-monthly moving average, this even increases to $R = 0.85$. Figure 6b shows that about half the increase in ASR is driven by changes in clouds, whereas the other half is driven by other causes, mainly changes in surface albedo and aerosols. In Fig. 6c, the residuals are shown, which have a trend of $0.37 \pm 0.06\ \mathrm{Wm^{-2}}$ per decade over the entire period. The data shows break points as well. There appears to be a large jump in March 2016 when MODIS C61 replaced MODIS C5 for input of cloud properties. When using BEAST on these residuals, it shows a break point with probability 1 from June to July 2001 and a break point with probability 1 from February to March 2016. We do not really know a reason for a break around July 2001. However, the Aqua measurements started in July 2002, which may have caused a change, so we placed the first break point there. The break point from February to March 2016 is most likely due to the fact that MODIS C61 replaces MODIS C5 so we keep the break point there.

https://doi.org/10.5194/egusphere-2025-418
Preprint. Discussion started: 24 February 2025

We again split the period into smaller pieces split by break points. Since the period until June 2002 is too short to draw any relevant conclusions, we examined the periods July 2002 until February 2016 and March 2016 until December 2021 (Fig. 6d). The period from July 2002 until February 2016 gives a total trend of 0.3 ± 0.1 Wm^{-2} per decade, while the trend over the second period March 2016 until December 2021 is -0.61 ± 0.43 Wm^{-2} per decade. As for the clear-sky OLR from CERES, the potential break has considerable implications for corresponding trend estimates.

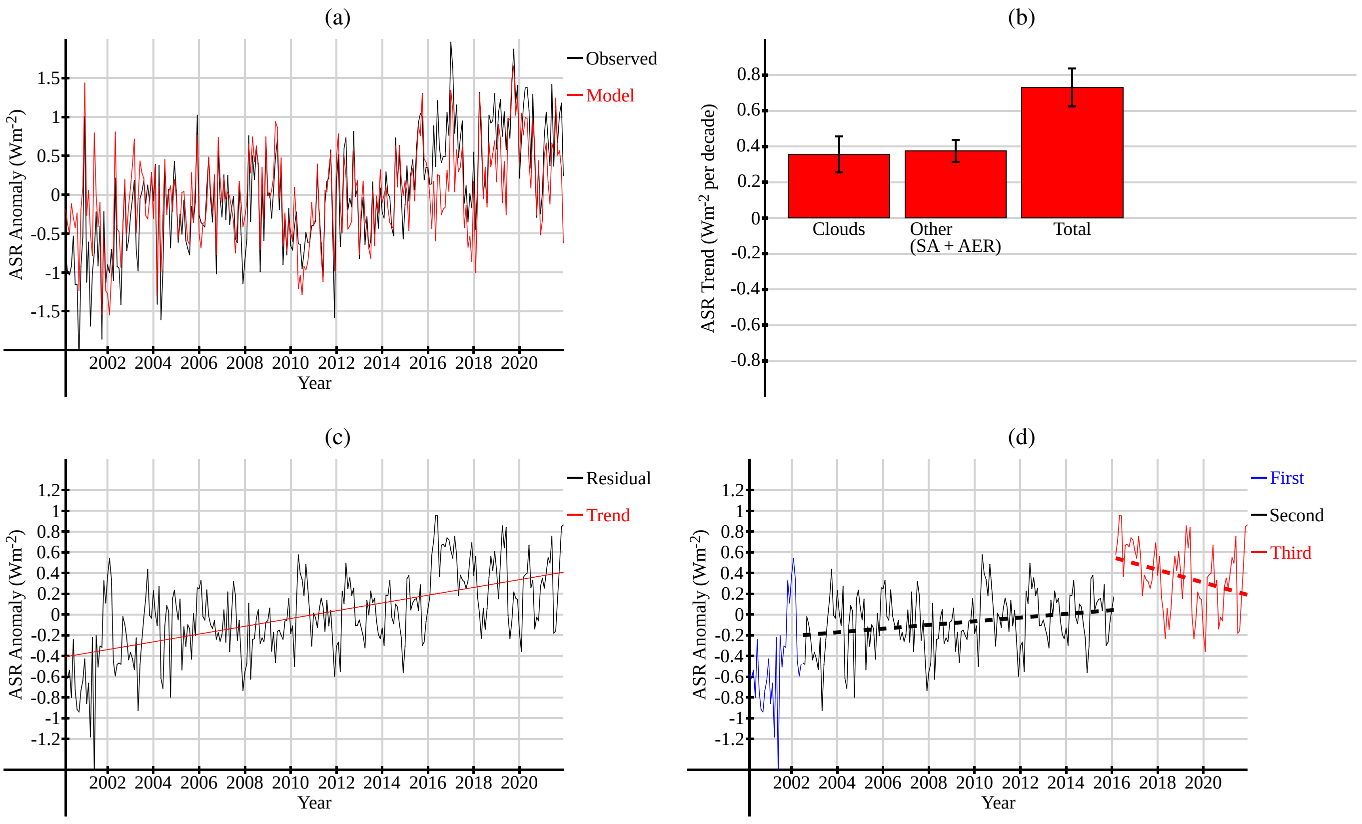

Figure 6. As Fig. 5 but for ASR.

5.2 Regression with cloud cover from ISCCP

The cloud data from ISCCP is used to estimate the cloud effect on OLR from March 2000 to June 2017, and results are shown in Fig. 7. From Fig. 7a it is clear that the regression model in this case does not perform well: the monthly fluctuations are much larger in the observed OLR than in the modeled OLR and only at longer time scales, the modeled OLR agrees with the observations. This is also visible in the low R of 0.49. When we take the 12-monthly moving average, it improves to $R = 0.66$. Figure 6b shows what the increase in OLR is distributed between the different factors. Clouds and temperature contributed both

https://doi.org/10.5194/egusphere-2025-418
Preprint. Discussion started: 24 February 2025

about half of the total increase, whereas other factors (mainly greenhouse gases) have not really contributed. The residuals are depicted in Fig. 7c with trend $-0.01 \pm 0.12\ \mathrm{Wm^{-2}}$ per decade.

The ISCCP data appear to have a large inhomogeneity in 2012 which can be directly related to a jump in the cloud cover data (see Fig. A1 in the appendix for a better overview). The residuals before 2002 seem to be lower than after 2002, but this is less clearly visible in the cloud cover data. Using BEAST on these residuals also gave a break point from October to November 2001 with probability 0.83 and a break point from January to February 2012 with probability 0.67. This is consistent with the analysis of the ISCCP cloud data in the appendix. Given the large inhomogeneity in January 2012 in the cloud data of ISCCP, we assume that the second break point is from December 2011 to January 2012. The first break point is less clear. For both break points, we do not have an explanation.

In Fig. 7d, we examined the periods January 2002 until December 2011 and January 2012 until June 2017, since the period until December 2001 is too short to give any meaningful results. The trend over the period from January 2002 to December 2011 is $-0.12 \pm 0.25\ \mathrm{Wm^{-2}}$ per decade and the trend over the second period from January 2012 to June 2017 is $0.95 \pm 0.55\ \mathrm{Wm^{-2}}$ per decade.

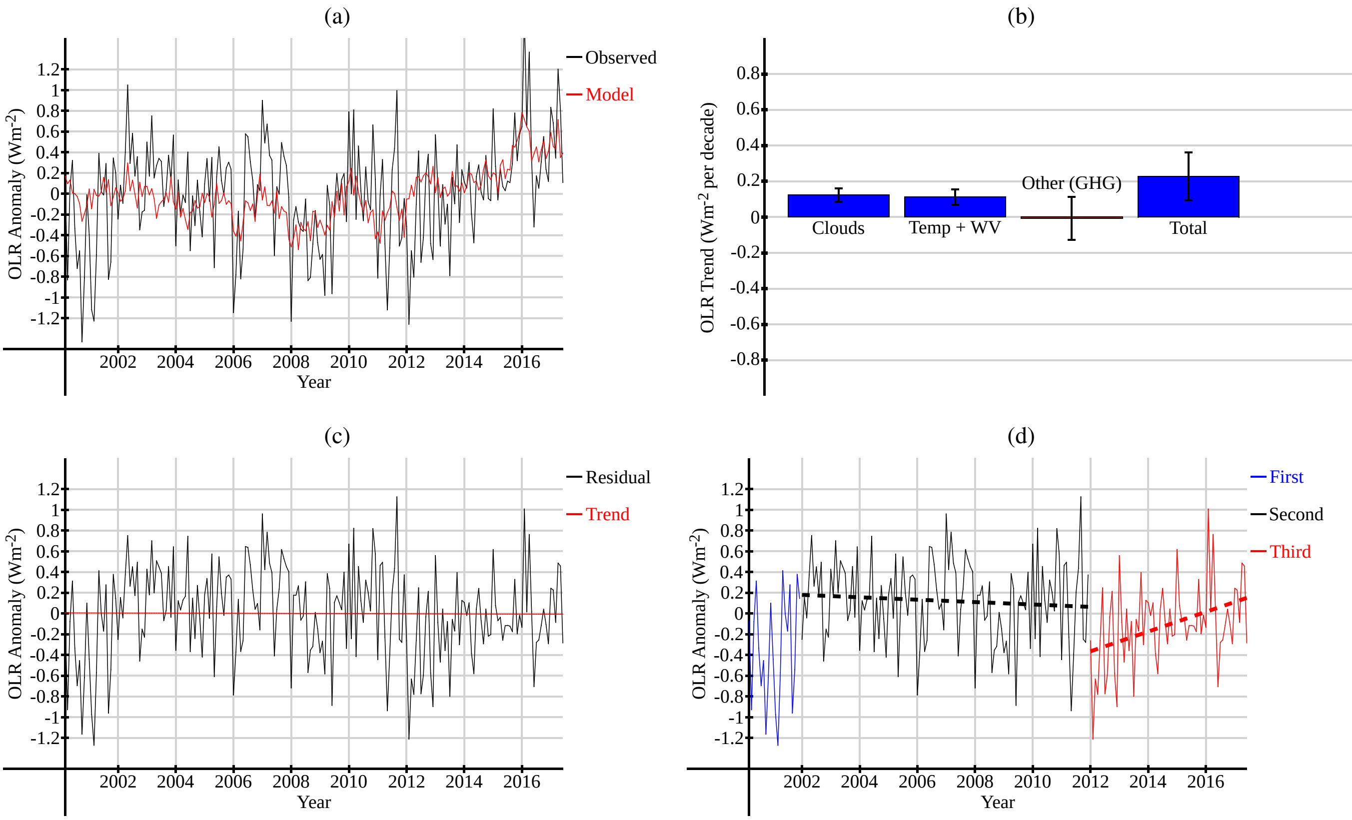

Figure 7. Explaining OLR with the cloud data from ISCCP for the cloud effect from March 2000 to June 2017: (a) compares the regression model with the observed OLR; (b) attributes the trend in OLR to different drivers; (c) shows the complete residuals; (d) illustrates the possible break points in January 2012 and 2002.

Fig. 8 shows the results when we use the ISCCP cloud cover to estimate the cloud effect on ASR from March 2000 to June 2017. Here the regression model seems slightly better than when explaining the OLR, which is also visible in $R = 0.64$. When taking the 12-monthly moving average, the correlation increases to $R = 0.68$. Figure 8b shows that clouds contributed slightly more than half of the increase in ASR and the other half was caused by other factors (mainly surface albedo and aerosols). The residuals are depicted in Fig. 8c with trend $0.31 \pm 0.13\ \mathrm{Wm^{-2}}$ per decade. There seems to be a trend break in 2012 but there is no clear jump, probably because ISCCP total cloud cover is relatively stable, as jumps in cloud cover at different heights partially cancel each other out. Until 2002, the residuals are higher, although we do not know a particular reason for this. We also used BEAST on these residuals to detect break points. BEAST found a strong break point from August to September 2002 with probability 0.84. The inhomogeneity in 2012 is less clear with probability 0.25, probably because it is not really a jump but more a trend break. We do not know what causes these possible inhomogeneities.

https://doi.org/10.5194/egusphere-2025-418
Preprint. Discussion started: 24 February 2025

We also split up the residuals between the different periods and calculated trends separately. We examined the periods January 2003 until December 2011 and January 2012 until June 2017 in Fig. 8d. The first period has a trend of $-0.59 \pm 0.3\ \mathrm{Wm^{-2}}$ per decade and the second period has total trend $1.06 \pm 0.53\ \mathrm{Wm^{-2}}$ per decade. There does not seem to be a jump in January 2012, but there is a clear trend break.

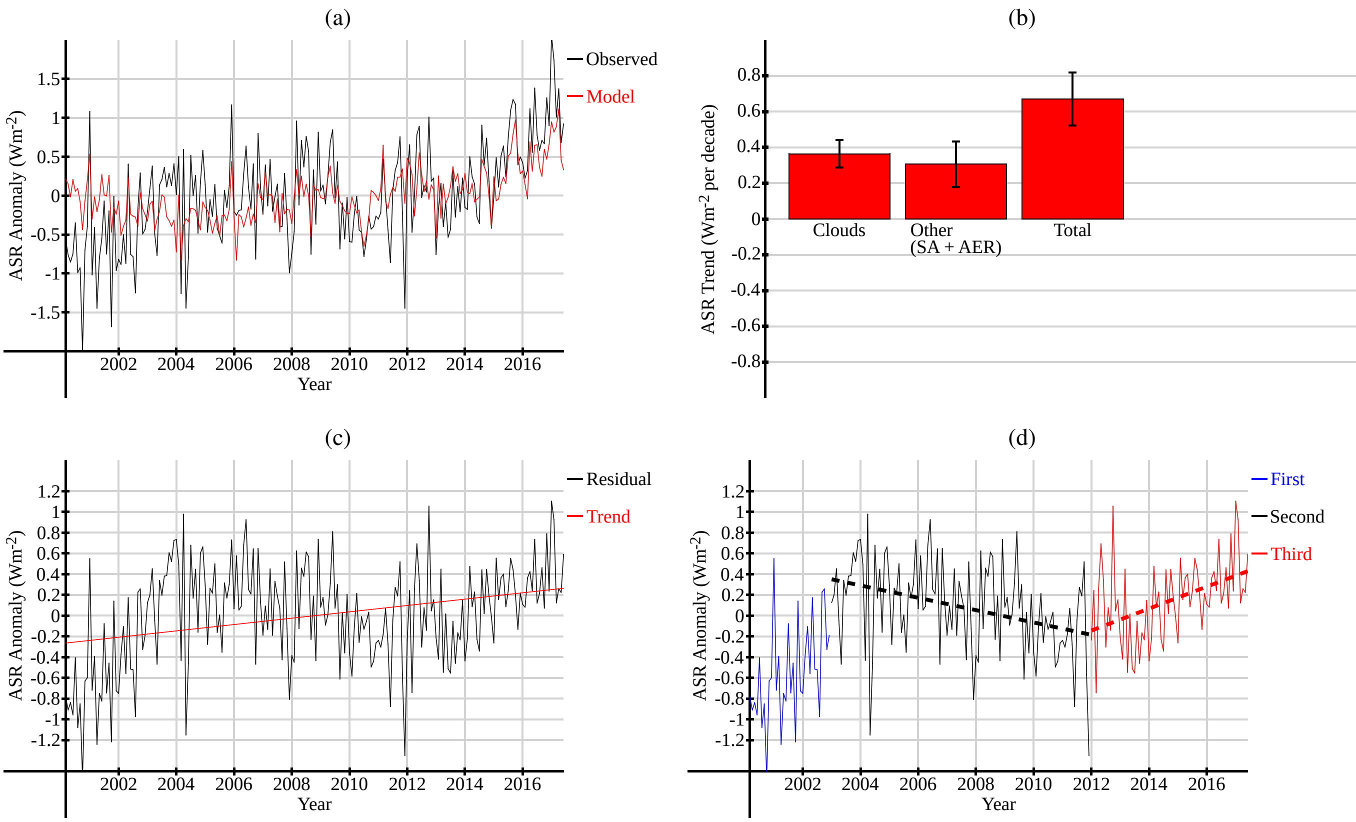

Figure 8. As Fig. 7 but for ASR.

5.3 Regression with cloud cover from CLARA-A3

When the cloud data from CLARA-A3 is used to estimate the cloud effect on OLR from March 2000 to December 2020, results are as displayed in Fig. 9. The regression model seems to work rather well with $R = 0.7$ as it explains most of the monthly fluctuations. When taking the 12-monthly moving average, the correlation even increases to $R = 0.8$. Only at the start, the model is clearly off, which can also be seen in the residuals. Figure 9b shows how much each factor contributes to the increase in OLR. Mainly the increase in temperature has caused the increase in OLR whereas clouds led to a slight increase in OLR which was counteracted by a decrease from other factors (mainly greenhouse gases). In Fig. 9c, the residuals are depicted with a total trend $-0.11 \pm 0.07\ \mathrm{Wm^{-2}}$ per decade. The high values before 2003 are probably related to positive anomalies

https://doi.org/10.5194/egusphere-2025-418
Preprint. Discussion started: 24 February 2025

in CLARA-A3 high cloud cover, as shown in Appendix Fig. A2. Using BEAST, we get a break point from March to April 2001 with probability 0.99 and a break point from September to October 2002 with probability 0.88. We thus assume that the period before 2003 is not entirely homogeneous and mainly focus on the period from 2003 onward, in which no further inhomogeneities are identified. The total trend over this period is $-0.09 \pm 0.08\ \mathrm{Wm}^{-2}$ per decade (Fig. 9d).

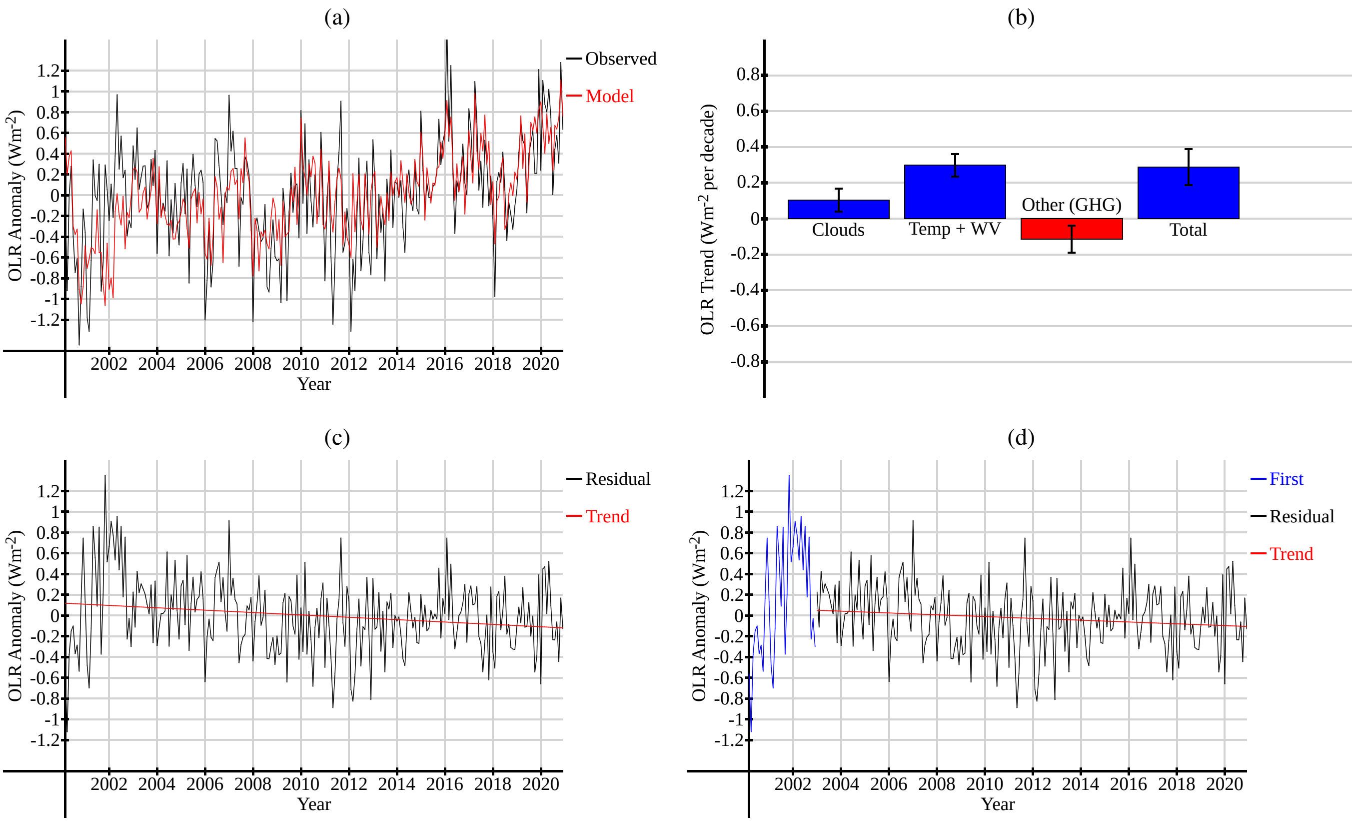

Figure 9. Explaining OLR with the cloud data from CLARA-A3 for the cloud effect from March 2000 to December 2020: (a) compares the regression model with the observed OLR; (b) attributes the trend in OLR to different drivers; (c) shows the complete residuals; (d) illustrates the homogeneous period from 2003 onward.

Regression results using the cloud data from CLARA-A3 to estimate the cloud effect on ASR are shown in Fig. 10. The regression model misses most of the increasing trend, and although the monthly fluctuations are partly reproduced, the R is low (0.56). For the 12-monthly moving average, it even decreases to $R = 0.44$. Figure 10b shows that (in this analysis) changes in clouds only contributed a little bit to the increase in ASR and other factors (mainly surface albedo and aerosols) should thus have caused almost the entire increase. In Fig. 10c, the residuals are depicted with total trend $0.67 \pm 0.09\ \mathrm{Wm}^{-2}$ per decade. There does not seem to be a clear inhomogeneity in 2003, although the outlier November 2001 is remarkable. This is probably

https://doi.org/10.5194/egusphere-2025-418
Preprint. Discussion started: 24 February 2025

a result from the outlier in the mid-level cloud coverage in November 2001 (Appendix Fig. A2). There also seems to be a small dip between 2009 and 2012 and a fast increase after 2012 that drives the trend. No clear breaks are visible. When running BEAST, it only finds a possible break point from June to July 2009 with probability 0.49 which marks the start of the peak. Figure A7 in the appendix shows that the low cloud cover of CLARA-A3 has a clear dip too between 2009 and 2012 compared to CERES SSF cloud cover. That dip in low cloud cover is most likely the cause of the dip in the residuals here.

Since the period before 2003 is probably not completely homogeneous, we show a separate trend estimate from January 2003 onward in Fig. 10d. The trend over this shorter period is $0.75 \pm 0.11\ \mathrm{Wm}^{-2}$ per decade.

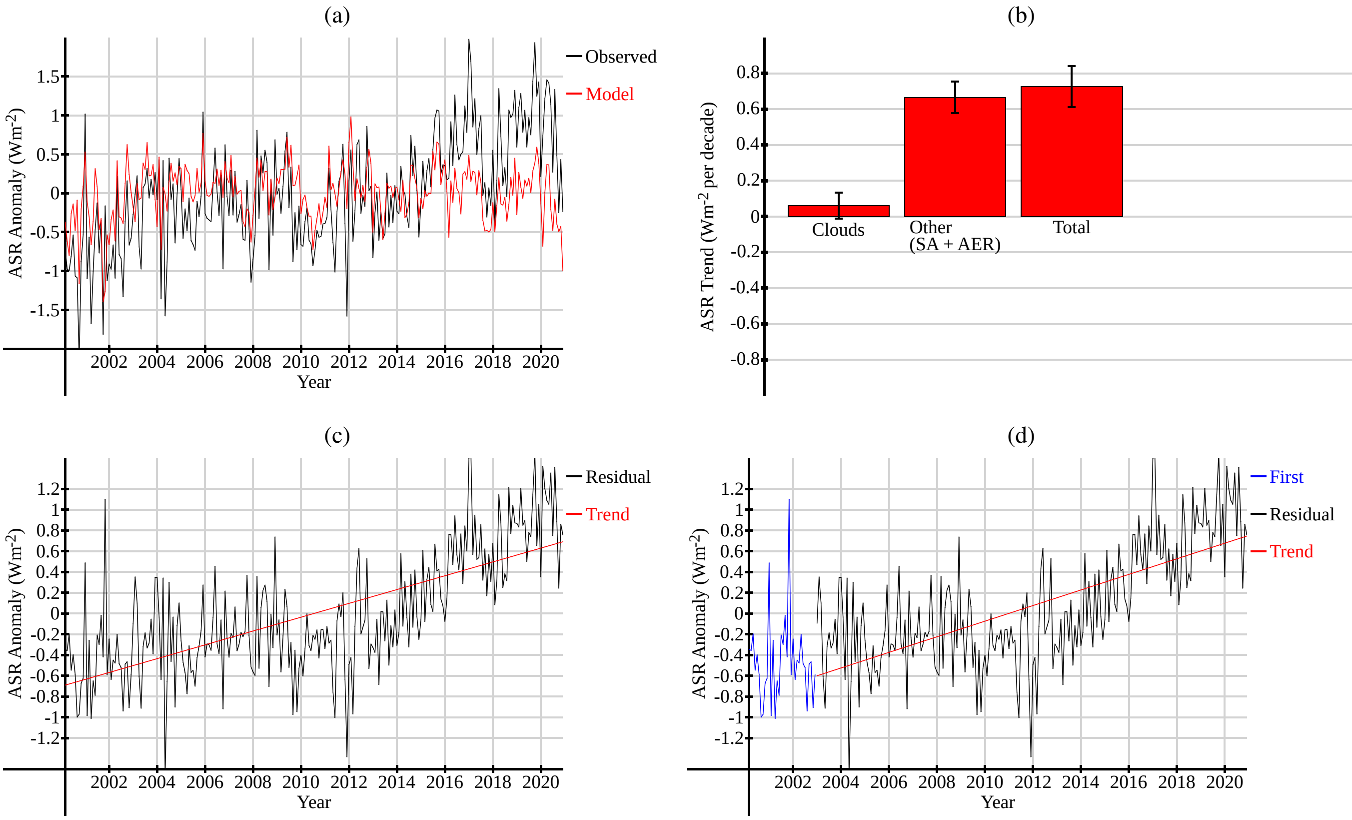

Figure 10. As Fig. 9 but for ASR.

5.4 Regression with cloud cover from CERES SSF

Finally, Fig. 11 shows the results when we use the CERES SSF cloud data to estimate the cloud effect on OLR from July 2002 to December 2021. We see that the regression model works rather well with $R = 0.78$ and it also explains the monthly fluctuations relatively well. When we take the 12-monthly moving average, the correlation even increases to $R = 0.85$. Only approximately from 2014 to 2016, the model is a bit off. Figure 11b shows how the increase in OLR is distributed over the different causes. The increase in temperature led to a strong increase in OLR, whereas cloud cover changes led to a slight decrease. As a result, the remaining other factors (mainly greenhouse gases) have led to a non-significant increase in OLR. The residuals are shown in Fig. 11c with trend $0.06 \pm 0.07\ \mathrm{Wm}^{-2}$ per decade. The peak from around 2014 until 2016 is probably a result of the high values for the mid-high-level cloud coverage from Terra (see Fig. A3 in the appendix), especially on the day-night cloud cover and not so much on the day-only cloud cover (see Fig. A3 and A4 in the appendix). The mid-high cloud cover from Terra is higher than from Aqua until March 2016, while after March 2016 the two cloud products are more similar (not shown). In the appendix in Fig. A7, we also see that the high cloud cover from CERES peaks in this period compared to the high cloud cover of CLARA-A3. BEAST detects two break points around this peak, one from December 2012 to January 2013 with probability 0.83 and the other from May to June 2016 with probability 0.78. The second break point is probably due to the transit from MODIS C5 to MODIS C61 in March 2016. When we visually compared the Terra and Aqua mid-high cloud cover, we clearly saw a break point at the end due to the transit from MODIS C5 to MODIS C61, but we found a more gradual one starting in 2010 with no clear jump. As such, we have no clear explanation for the start of the peak.

Other than this peak, there do not seem to be many inhomogeneities. In Fig. 11d the residuals are split into two periods: the first period starts in July 2002 and ends in February 2016 and the second period start in March 2016 and continues until December 2021. Corresponding trends are $0.18 \pm 0.12\ \mathrm{Wm}^{-2}$ per decade and $-0.18 \pm 0.38\ \mathrm{Wm}^{-2}$ per decade, respectively. There is no strong jump but there is rather a peak in residuals from 2014 until 2016. That peak drives the trend in the first period, while in total no clear trend is visible in the OLR residuals if they are calculated using cloud data from CERES SSF.

https://doi.org/10.5194/egusphere-2025-418
Preprint. Discussion started: 24 February 2025

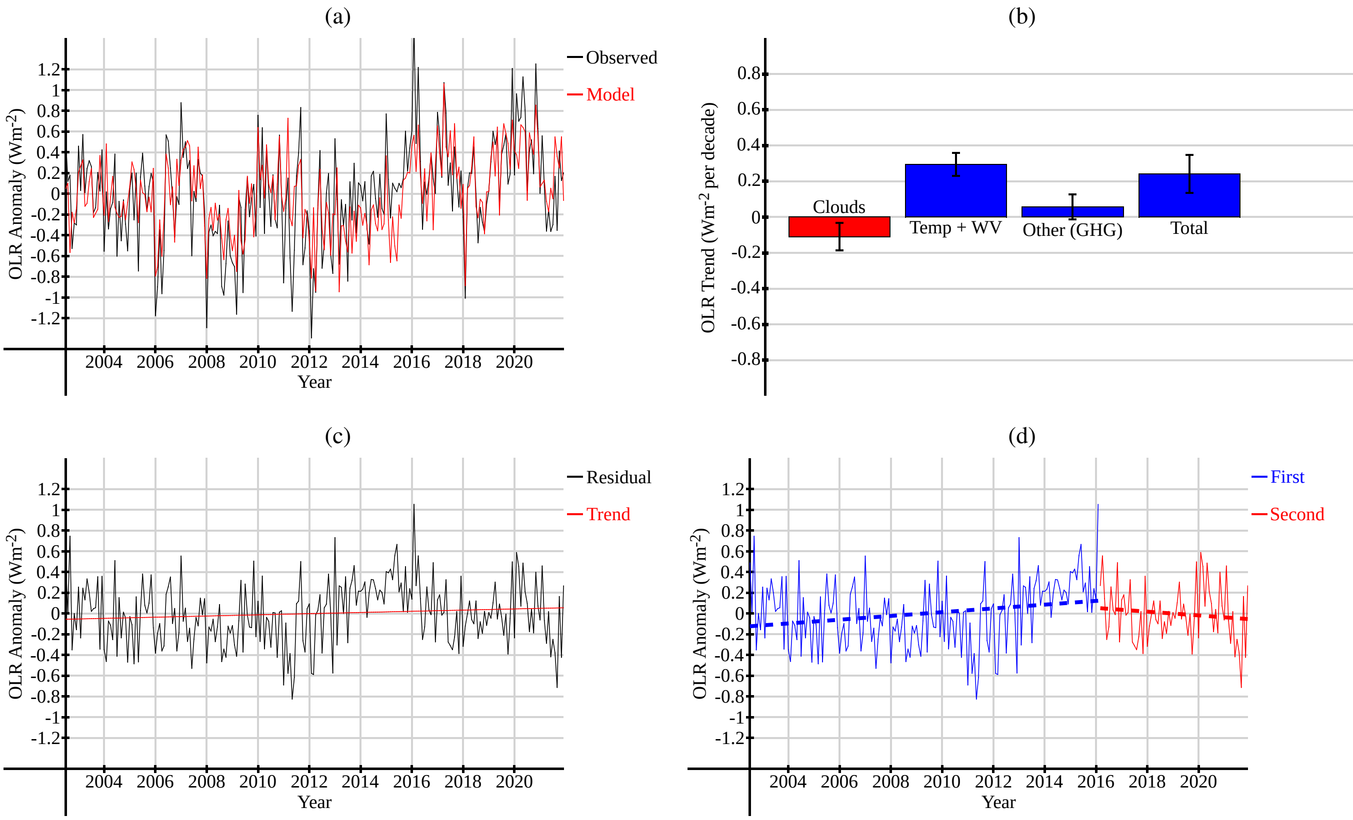

Figure 11. Explaining OLR with the cloud data from CERES SSF for the cloud effect from July 2002 to December 2021: (a) compares the regression model with the observed OLR; (b) attributes the trend in OLR to different drivers; (c) shows the complete residuals; (d) illustrates the possible break point in March 2016.

In Fig. 12 the results using the day-time CERES SSF cloud data to estimate the cloud effect on ASR are displayed. The regression model seems to work rather well in this case too with $R = 0.77$. When taking the 12-monthly moving average, the correlation increases to $R = 0.79$. The monthly fluctuations are also reproduced relatively well and only at the very end, the model is a bit off. Figure 12b illustrates the contribution of each factor to the increase in ASR. In this analysis, clouds only contributed slightly to the increase in ASR (about 30 %) and the main cause is other factors (mainly surface albedo and aerosol changes). The residuals are also depicted with trend $0.49 \pm 0.07\ \mathrm{Wm^{-2}}$ per decade. There seems to be a slowly increasing trend until 2016. From then onward, there appear to be two plateaus separated by September 2018. An inhomogeneity might also be present in March 2016 due to the change in MODIS processing. The possible jump in March 2016 is not very large, but the jump in September 2018 is considerably larger. When using BEAST on these residuals, it finds a break point from August to September 2018 with probability 0.36. BEAST does not really detect the break point in March 2016 (it finds a probability of 0.11), probably since the jump is relatively small. We have no clear idea why there should be a break point in September 2018.

https://doi.org/10.5194/egusphere-2025-418
Preprint. Discussion started: 24 February 2025

In Fig. 12d, the residuals are split over the three periods separated by March 2016 and September 2018. The total trend over the first period is $0.3 \pm 0.12\ \mathrm{Wm^{-2}\ per\ decade}$ and the middle and final period are too short for any sensible trend estimate.

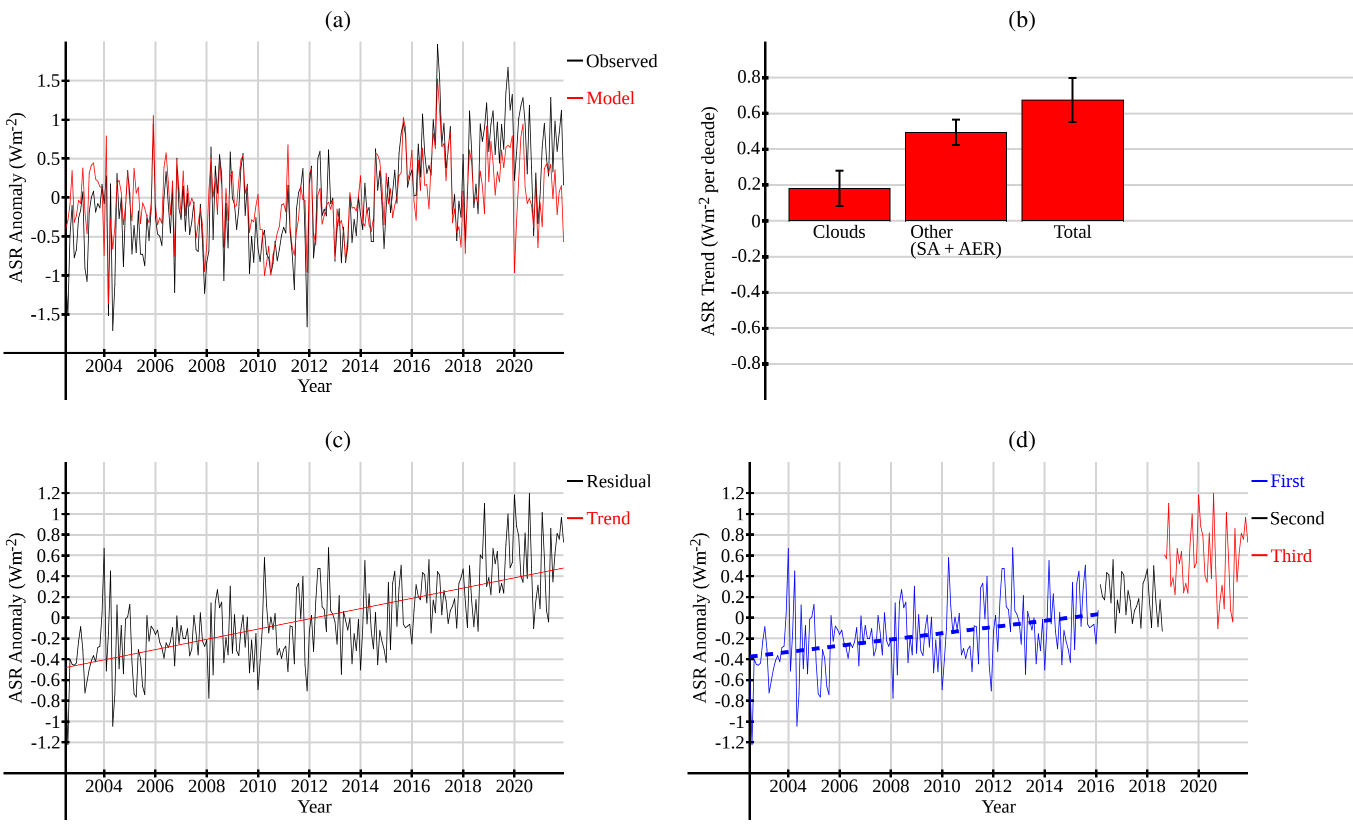

Figure 12. As Fig. 11 but for ASR.

6 Discussion

In this section, some limitations of our methods are discussed. We used linear regression to estimate the effects of cloud coverage and temperature on OLR and ASR and worked with global averages. The main assumptions for the linear regression are:

- Cloud coverage in a specific height range (low, medium, high) is linearly related to Q, where Q denotes either OLR or ASR.

- Temperature (in the lower troposphere) is linearly related to $Q^{\frac{3}{4}}$, where Q denotes OLR.

https://doi.org/10.5194/egusphere-2025-418
Preprint. Discussion started: 24 February 2025

The first assumption implies that the influence of clouds on TOA radiation depends only on the height bin. However, this is not necessarily the case. In general, the mean height of clouds within a bin can change, which will impact their radiative effects. In addition, especially for ASR the cloud optical depth is important, but changes in cloud optical depth are not taken into account. The second assumption comes directly from theoretical considerations, although the LT temperature has its limitations as a proxy for the radiative temperature. In addition we assume that the water vapour feedback is linear in temperature.

Regarding the use of global averages, we assume that the sum of regional impacts of temperature and clouds on TOA radiation can be approximated by the impact of the (weighted) global mean temperature and clouds on TOA radiation. This is a valid assumption if the radiation dependence on temperature and clouds is indeed linear.

In Fig. 13, the OLR regression results from all methods are compared with the observed OLR from CERES. As outlined before, all methods apart from ISCCP reproduce the monthly variations in OLR relatively well. The long-term trends predicted by the different methods are partly in good agreement with the observations, resulting in small residual trends (Table 3). In particular, the model based on CERES Clear-Sky data yields a larger increase in (all-sky) OLR than observed (i.e. negative residual trend) (see Table 3 or Fig. 14 for an overview). However, after correction for potential breaks in the time series, the residual trends become much smaller. Overall, we conclude that the OLR regression models reproduce the observed all-sky OLR reasonably well.

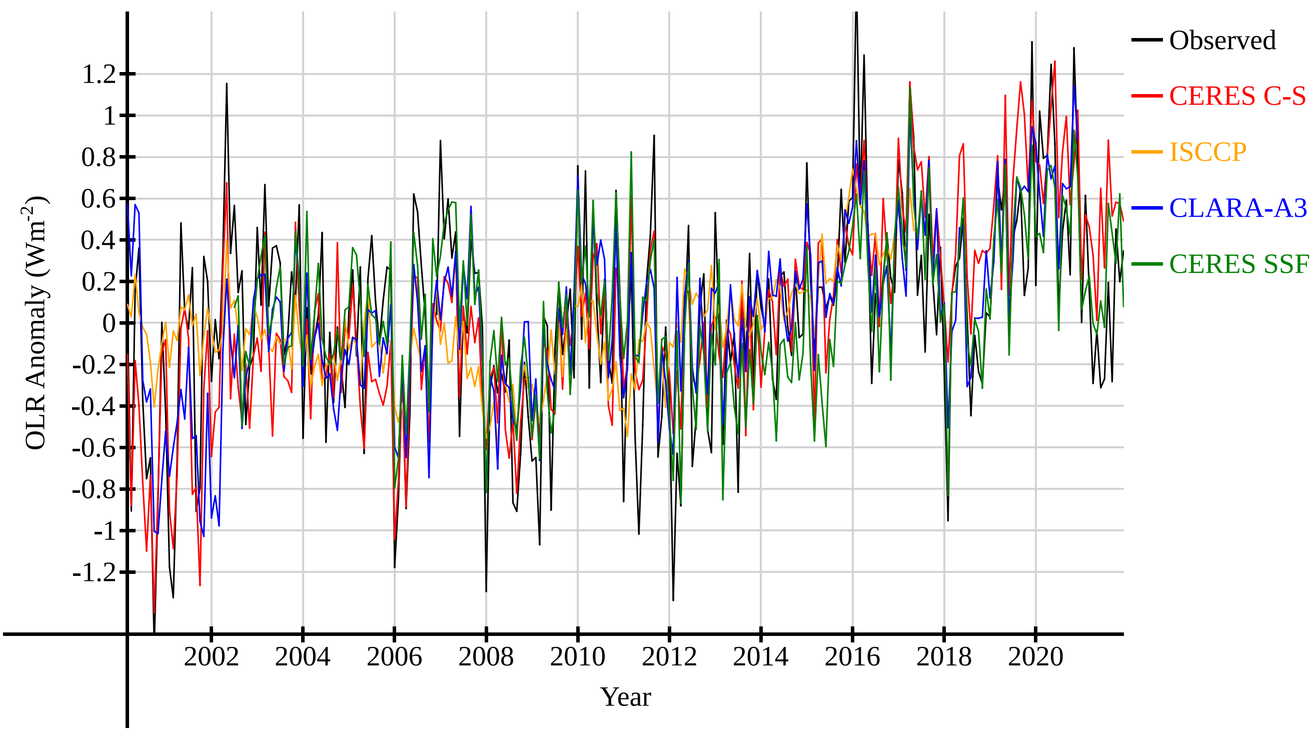

Figure 13. Comparison of the different regression models with the observed OLR. CERES C-S stands for CERES Clear-Sky.

https://doi.org/10.5194/egusphere-2025-418
Preprint. Discussion started: 24 February 2025

Method	Other (GHG) OLR Trend	Other (GHG) OLR Trend per decade between likely breakpoints
CERES C-S	-0.27 ± 0.06 Wm^{-2}	-0.05 ± 0.29 Wm^{-2} , 0.18 ± 0.26 Wm^{-2}, -0.36 ± 0.43 Wm^{-2}
ISCCP	-0.01 ± 0.12 Wm^{-2}	-0.12 ± 0.25 Wm^{-2}, 0.95 ± 0.55 Wm^{-2}
CLARA-A3	-0.11 ± 0.07 Wm^{-2}	-0.09 ± 0.08 Wm^{-2}
CERES SSF	0.06 ± 0.07 Wm^{-2}	0.18 ± 0.12 Wm^{-2}, -0.18 ± 0.38 Wm^{-2}

Table 3. Residual OLR trends found by the different methods and datasets over their entire period. The first column gives the uncorrected trends and the second column lists the trends between the suspected break points.

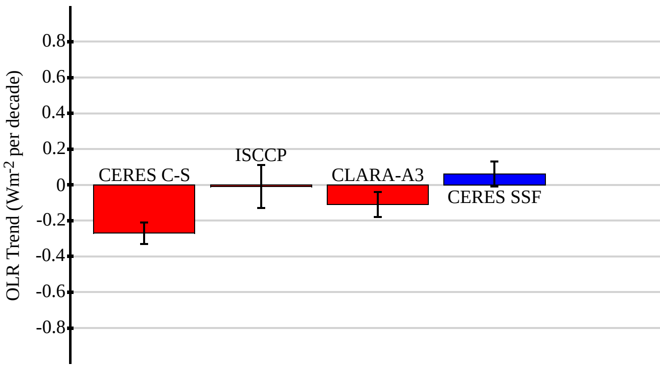

Figure 14. The Other (GHG) trends found by the different methods without correcting the possible break points.

Figure 15 compares all predictions of ASR with the observed ASR. As explained in the previous sections, the monthly variations can partly be reproduced. This indicates that clouds are the dominant forcing for monthly variations in ASR. We do not expect SA or AER to contribute much to the monthly variations. However, the observed long-term increase in ASR is not reproduced consistently by the different models, probably because there are more suspect inhomogeneities in the low cloud cover and because the cloud effect on ASR is larger than on OLR. Moreover, ASR varies more between clouds at the same height due to variations in cloud optical depth. Changes in cloud cover probably strongly contributed to the increase in ASR, but is hard to give a precise number based on our regressions.

https://doi.org/10.5194/egusphere-2025-418
Preprint. Discussion started: 24 February 2025

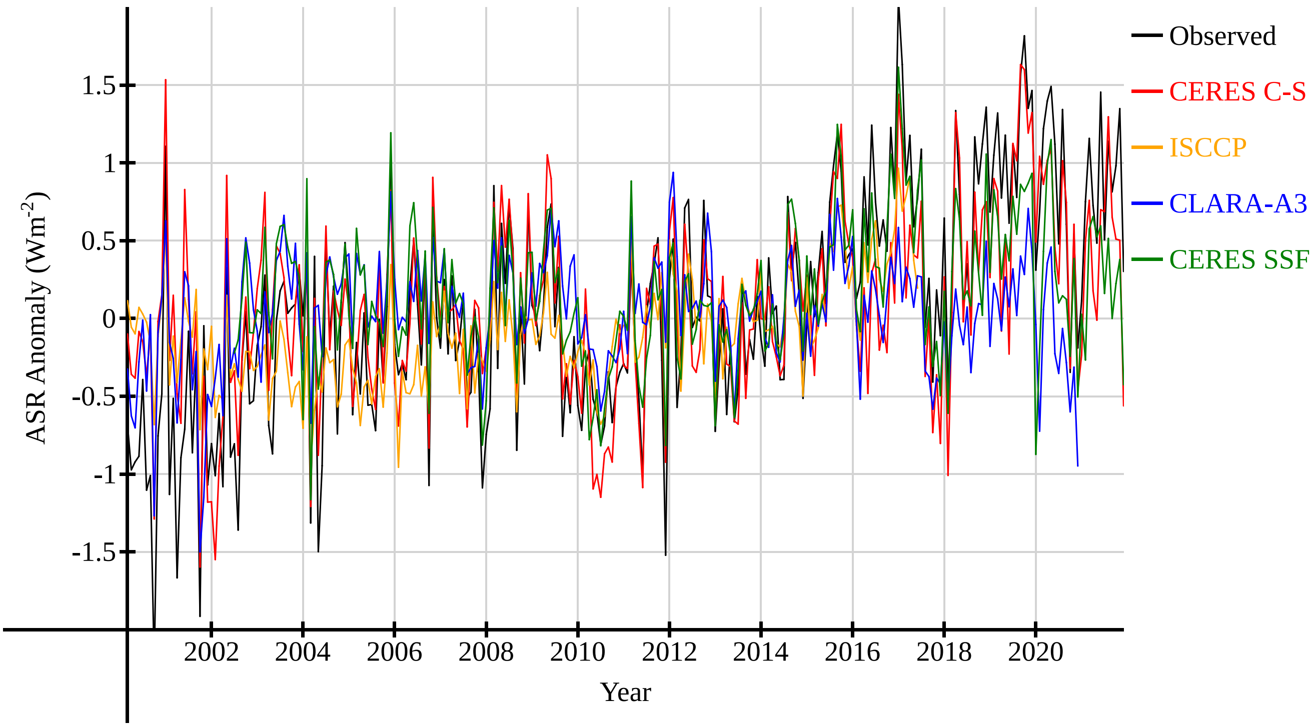

Figure 15. As Fig. 13 but for ASR.

Method	Other (SA + AER) ASR Trend	Other (SA + AER) ASR Trend per decade between likely breakpoints
CERES C-S	$0.37 \pm 0.06\ \mathrm{Wm^{-2}}$	$0.3 \pm 0.1\ \mathrm{Wm^{-2}},\ -0.61 \pm 0.43\ \mathrm{Wm^{-2}}$
ISCCP	$0.31 \pm 0.13\ \mathrm{Wm^{-2}}$	$-0.59 \pm 0.3\ \mathrm{Wm^{-2}},\ 1.06 \pm 0.53\ \mathrm{Wm^{-2}}$
CLARA-A3	$0.67 \pm 0.09\ \mathrm{Wm^{-2}}$	$0.75 \pm 0.11\ \mathrm{Wm^{-2}}$
CERES SSF	$0.49 \pm 0.07\ \mathrm{Wm^{-2}}$	$0.3 \pm 0.12\ \mathrm{Wm^{-2}}$

Table 4. As Table 3 but for residual ASR trends.

https://doi.org/10.5194/egusphere-2025-418
Preprint. Discussion started: 24 February 2025

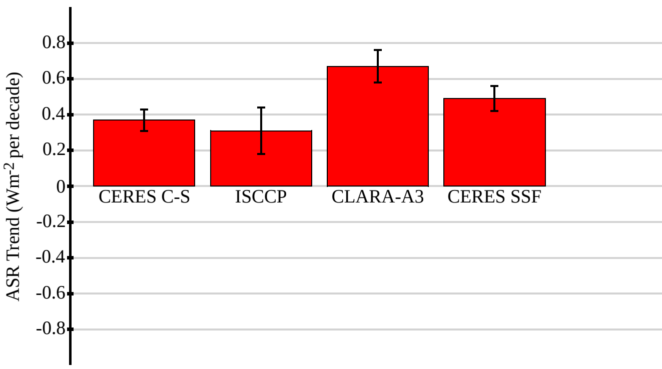

Figure 16. As Fig. 14 but for ASR.

We expected to find a monotonous decrease in residual OLR, because GHG have increased monotonously. However, a decrease in residual OLR is only obtained when using CERES Clear-Sky data to estimate the cloud effect, and this decrease is not monotonous, as is evident in Table 3, which summarizes the trends between likely breaks. This is in contrast to the scientific consensus, in which a decrease in OLR of approximately $0.4\ \mathrm{Wm}^{-2}$ per decade over 2000 until 2020 due to the increase in greenhouse gases is expected (Dentener et al., 2021). This value is virtually certain according to the IPCC and has been calculated using physical models. Loeb et al. (2021) estimate a decrease in OLR due to greenhouse gases of $0.2\ \mathrm{Wm}^{-2}$ per decade, but the underlying analysis method may have been affected by breaks in the input datasets.

Loeb et al. (2021) find an OLR increase due to temperature and water vapour of around $0.3\ \mathrm{Wm}^{-2}$ per decade in the period September 2002 to March 2020. Our estimated effect of temperature and water vapour during the same period is approximately $0.32 \pm 0.08\ \mathrm{Wm}^{-2}$ per decade when using CERES SSF for the cloud data and $0.37 \pm 0.09\ \mathrm{Wm}^{-2}$ per decade when using CLARA-A3 as cloud data, so both match rather well with Loeb et al. (2021). The effect when using CERES Clear-sky data for the cloud cover effect is around $0.2 \pm 0.05\ \mathrm{Wm}^{-2}$ per decade which is significantly smaller. However our estimated OLR trend due to clouds is larger than reported by Loeb et al. (2021) ($0.31 \pm 0.07\ \mathrm{Wm}^{-2}$ per decade versus approximately $0.15\ \mathrm{Wm}^{-2}$ per decade). This is probably because the temperature and water vapour effect on OLR differ for all-sky and clear-sky and we label this difference as cloud effect whereas Loeb et al. (2021) label this as temperature and water vapour effect. The combined effect of cloud cover, temperature and water vapour on OLR has a comparable trend in our analysis compared to Loeb et al. (2021). Also the combined effect of temperature and water vapour on OLR for 1 degree warming in our analysis is $1.63 \pm 0.27\ \mathrm{Wm}^{-2}$ when using CERES SSF as cloud data and $1.76 \pm 0.3\ \mathrm{Wm}^{-2}$ when using CLARA-A3 as cloud data compared to approximately $1.9\ \mathrm{Wm}^{-2}$ as estimated by the IPCC (Masson-Delmotte et al., 2023), so again our estimate is rather comparable with other studies. Because of these two agreements, we believe that this impact is modeled reliably. The OLR trend itself is also measured reliably (see Fig. 2), so the only possibly unreliably estimated parameter is the cloud effect. We considered two possible explanations why the cloud effect on OLR could be unreliably estimated in our analysis:

– The cloud effect on OLR is estimated incorrectly by the model because the regression coefficients are not correct.

https://doi.org/10.5194/egusphere-2025-418
Preprint. Discussion started: 24 February 2025

- The cloud effect on OLR is not completely proportional to the weighing factor and large systematic regional changes in cloud cover in combination with large differences in their effect create a trend in the cloud effect, without creating a trend in the global cloud cover.

Since temperature and water vapour approximately explain the observed trend in OLR, a negative trend in OLR due to greenhouse gases should be matched by a positive trend in OLR due to clouds. This could be realized by either a decrease in cloud fraction or height. Although cloud fraction has decreased slightly according to CERES SSF data (Fig. A3e), the high cloud fraction has increased (Fig. A3d), and it does not seem to be possible to obtain a positive OLR trend from these combined changes. Therefore, the first explanation does not appear to hold.

To test the second explanation, we performed additional regressions restricting the analysis to the tropics. These gave very similar results, in particular that the residual OLR also did not have a negative trend. Thus, although regional cloud changes might contribute to some uncertainty in the resulting global OLR trends, it is not an explanation for why our attribution fails to detect the expected larger contribution of the positive trend of GHG to OLR.

There may be other limitations of our method or artifacts in the observational datasets which can explain the partly unexpected results, but we are currently not aware of that.

7 Summary and conclusions

In this research, we analysed variations and trends in satellite observations of TOA radiative fluxes. The goal was to attribute changes in OLR and ASR to the different underlying causes. The effect of temperature and humidity on OLR was estimated by making regressions against UAH temperature data. Similarly, effects of clouds were estimated by regressions against various cloud cover datasets. The residual is due to factors not considered in the regressions, notably greenhouse gases. For ASR we considered regressions with cloud observations only and the residual is due to other factors like surface albedo and aerosols. A formal break detection algorithm was applied in order to detect possible inhomogeneities. A number of breaks were detected in the datasets and the most important ones are as follows.

We found that the TOA radiative fluxes showed a large spread before 2000. From 2000 onwards, likely breaks in various satellite datasets were detected which complicated the attribution. These breaks were mainly present in the cloud datasets, and consequently the results of cloud effects on trends in TOA fluxes were uncertain. In contrast, the effects of temperature and humidity on OLR appeared more accurate and consistent with other studies.

It is recommended that further research will be done into the likely breaks we detected, and to correct them in order to better attribute the all-sky radiative trends to the various causes.

The different regression models agreed relatively well on reproducing OLR but not so well on ASR. However, our attribution fails to detect the expected contribution of the positive trend of GHG to OLR. A number of possible explanations were discussed but we did not reach a final conclusion.

These analyses provide some new directions for future research. One option is to repeat this kind of analysis with homogenised cloud data. In addition, the cloud optical depth can be taken into account, which will probably improves the anal-

https://doi.org/10.5194/egusphere-2025-418
Preprint. Discussion started: 24 February 2025

ysis for ASR and perhaps OLR as well. Other factors like surface albedo and aerosols can also be taken into account. The attribution approach based on linear regression is relatively simple and can readily be applied to understand, intercompare and validate transient climate model simulations. Finally, an open question is why this attribution approach was unable to detect the expected decrease in OLR due to increasing greenhouse gases.

Data availability. CERES data were obtained from the NASA Langley Research Center CERES ordering tool at https://ceres.larc.nasa.gov/data/.
ISCCP cloud data can be downloaded via https://www.ncei.noaa.gov/products/international-satellite-cloud-climatology.
CLARA-A3 cloud data can be downloaded at https://wui.cmsaf.eu/safira/action/viewProduktDetails?eid=22277_22492&fid=40.
UAH temperature data can be donwloaded at https://www.nsstc.uah.edu/climate/index.html.

https://doi.org/10.5194/egusphere-2025-418
Preprint. Discussion started: 24 February 2025

Appendix A: Examination of cloud data

In the following sections, we examine the cloud data of ISCCP, CLARA-A3 and CERES SSF to search for inhomogeneities.

A1 Cloud data ISCCP

Figure A1 shows how the cloud coverage developed according to the data of ISCCP on all 3 heights and how the total cloud coverage developed. The data from the entire period July 1983 until June 2017 is shown. The low cloud coverage decreased very much with $-2.31 \pm 0.27\%$. The middle cloud coverage decreased a bit with $-0.65 \pm 0.23\%$, the high cloud coverage decreased with $-1.29 \pm 0.19\%$ and the total cloud cover decreased with as much as $-5.15 \pm 0.29\%$. The low, middle and high cloud cover have the same scale, but the total cloud cover has a larger scale. Before 2000, there are many inhomogeneities that we ignore for this paper. However in 2012, there is a large discontinuity that impacts our research. This jump shows up at all cloud heights and we do not know what caused it.

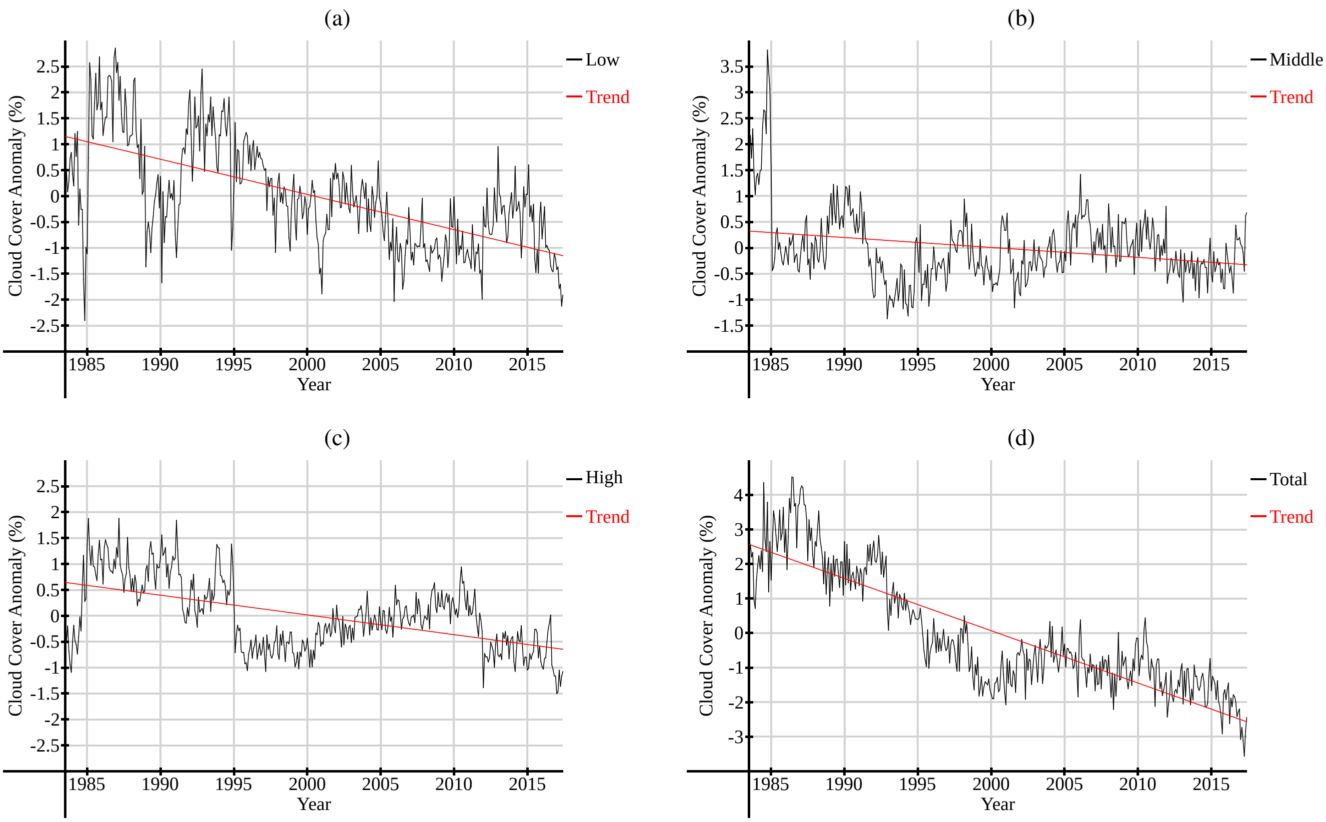

Figure A1. The cloud cover of ISCCP at all heights over the period July 1983 until June 2017: (a) contains the low cloud cover; (b) the middle cloud cover; (c) the high cloud cover; (d) the total cloud cover.

https://doi.org/10.5194/egusphere-2025-418
Preprint. Discussion started: 24 February 2025

460 ## A2 Cloud data CLARA-A3

Figure A2 shows the development of the cloud coverage at all 3 levels and the total cloud cover according to the CLARA-A3 data from March 1985 until December 2020. The trends are also added. The low cloud cover decreased with $-0.17 \pm 0.26\%$. The middle cloud cover even decreased with as much as $-1.51 \pm 0.11\%$, the high cloud cover decreased with $-1.2 \pm 0.29\%$ and the total cloud cover even decreased with $-2.98 \pm 0.32\%$. The low, middle and high cloud cover have the same scale as with 465 the ISCCP data, but the total cloud cover has a larger scale. Especially before 2000, there appear to be many inhomogeneities so we do not use these data in our paper. After 2000, there only seems to be an inhomogeneity at the very start in 2002 or 2003 in the middle and in particular in the high cloud cover which thus also shows up in the total cloud cover.

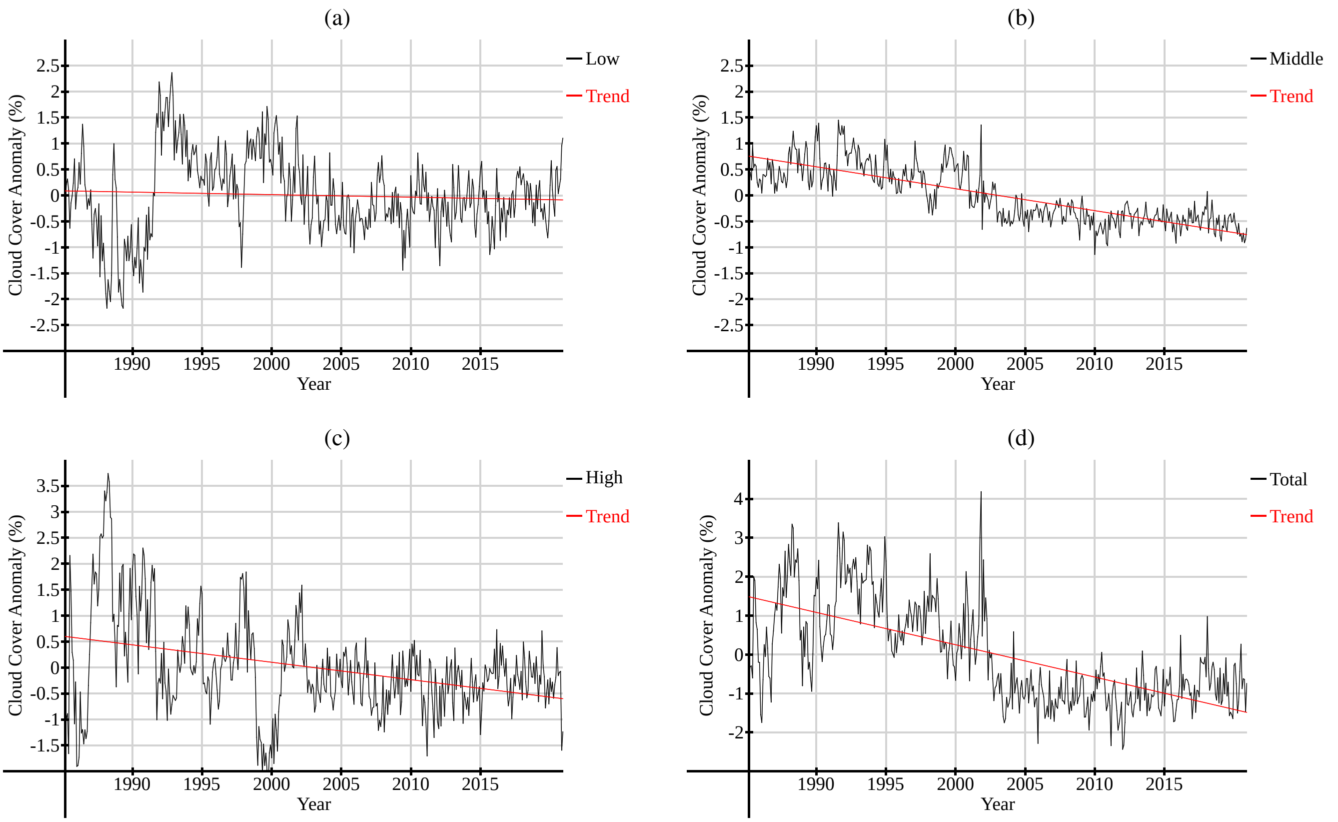

Figure A2. The cloud cover of CLARA-A3 at all heights over the period March 1985 until December 2020: (a) contains the low cloud cover; (b) the middle cloud cover; (c) the high cloud cover; (d) the total cloud cover.

https://doi.org/10.5194/egusphere-2025-418
Preprint. Discussion started: 24 February 2025

A3 Cloud data CERES SSF

Figure A3 shows the cloud cover at the 4 height levels according to the CERES SSF data during the day and night from July 2002 until February 2023. The trends are also added. The low cloud cover increased with $0.05 \pm 0.19\%$, the mid-low cloud cover decreased with $-0.61 \pm 0.08\%$, the mid-high cloud cover decreased with $-0.12 \pm 0.1\%$, the high cloud cover increased with $0.4 \pm 0.12\%$ and the total cloud cover decreased with $-0.28 \pm 0.19\%$. In low cloud cover, especially the jump in March 2016 stands out which drives the trend. This jump can mainly be found at the Terra data and does not seem to be there at the Aqua data. There also seems to be a bit of a dip between 2008 and 2010 in the low cloud cover, but this might just be noise. In the mid-low clouds, there are no clear jumps. In the mid-high clouds, there again seems to be a gradual decrease around March 2016 following a peak between 2012 and 2016. This pattern is again mainly visible at Terra. There do not seem to be inhomogeneities in the high cloud cover or in the total cloud cover.

https://doi.org/10.5194/egusphere-2025-418
Preprint. Discussion started: 24 February 2025

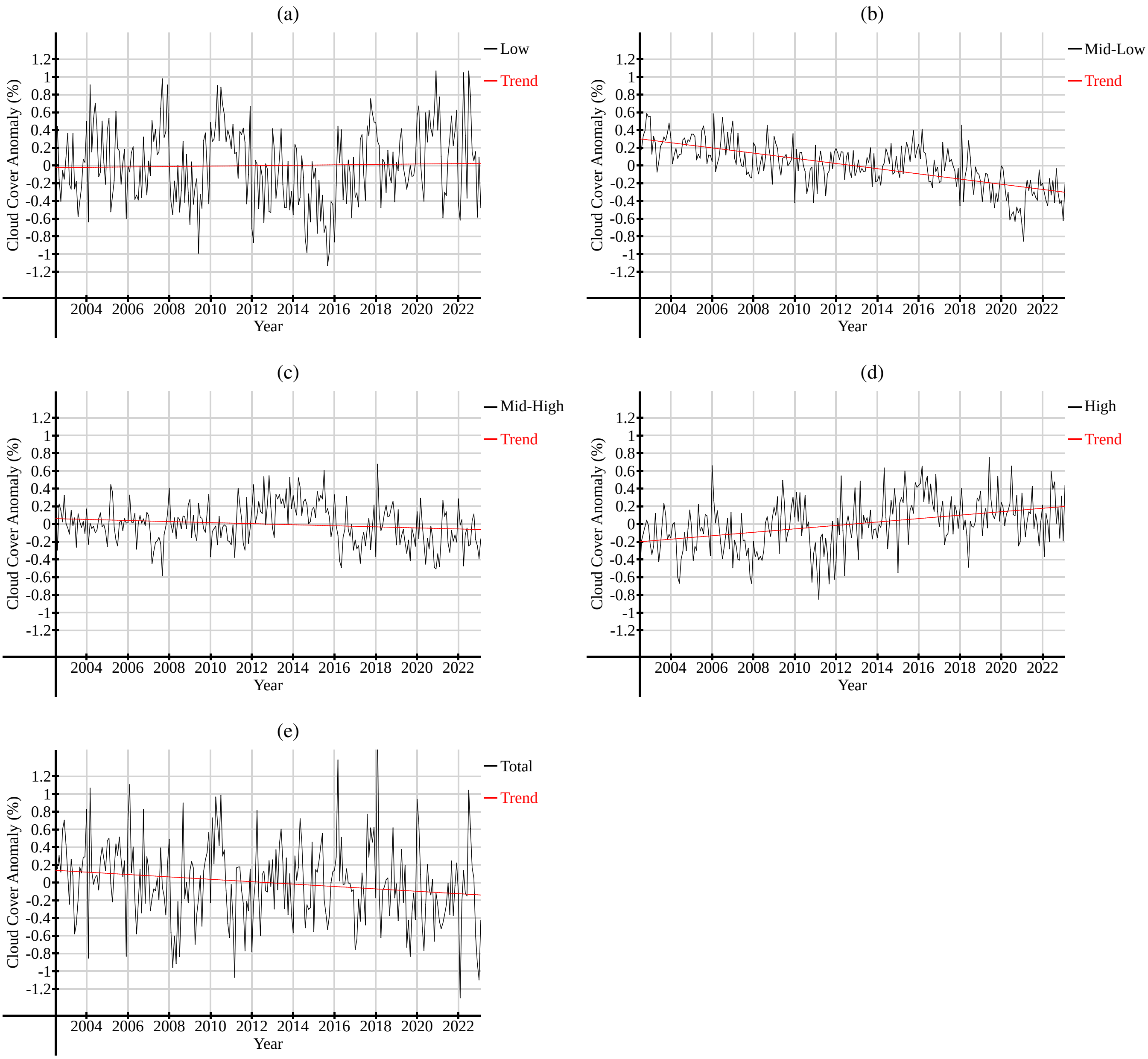

Figure A3. The cloud cover of CERES SSF during the day and night at all heights over the period July 2002 until February 2023: (a) contains the low cloud cover; (b) the mid-low cloud cover; (c) the mid-high cloud cover; (d) the high cloud cover; (e) the total cloud cover.

Figure A4 shows the same for the cloud cover at the 4 height levels during daytime only. The data is again everywhere shown from July 2002 until February 2023. We also added all trends. The low cloud cover decreased with $-0.1 \pm 0.19\%$, the mid-low cloud cover decreased with $-0.33 \pm 0.08\%$, the mid-high cloud cover decreased with $-0.22 \pm 0.1\%$, the high cloud

https://doi.org/10.5194/egusphere-2025-418
Preprint. Discussion started: 24 February 2025

cover increased with $0.42 \pm 0.09\%$ and the total cloud cover decreased with $-0.23 \pm 0.19\%$. The inhomogeneities of the cloud cover above are less clear here. There could be a small jump in the low cloud cover in March 2016, but it is very small. The dip between 2008 and 2010 also seems to be less pronounced. The mid-low cloud cover seems to be homogeneous. Just like with the mid-high cloud cover of the entire day, there seems to be a bit more mid-high clouds just before 2016 and a decrease afterwards. This pattern is less strong than with the cloud cover over the entire day. The high cloud data does not show any real inhomogeneities, just as the total cloud cover.

https://doi.org/10.5194/egusphere-2025-418
Preprint. Discussion started: 24 February 2025

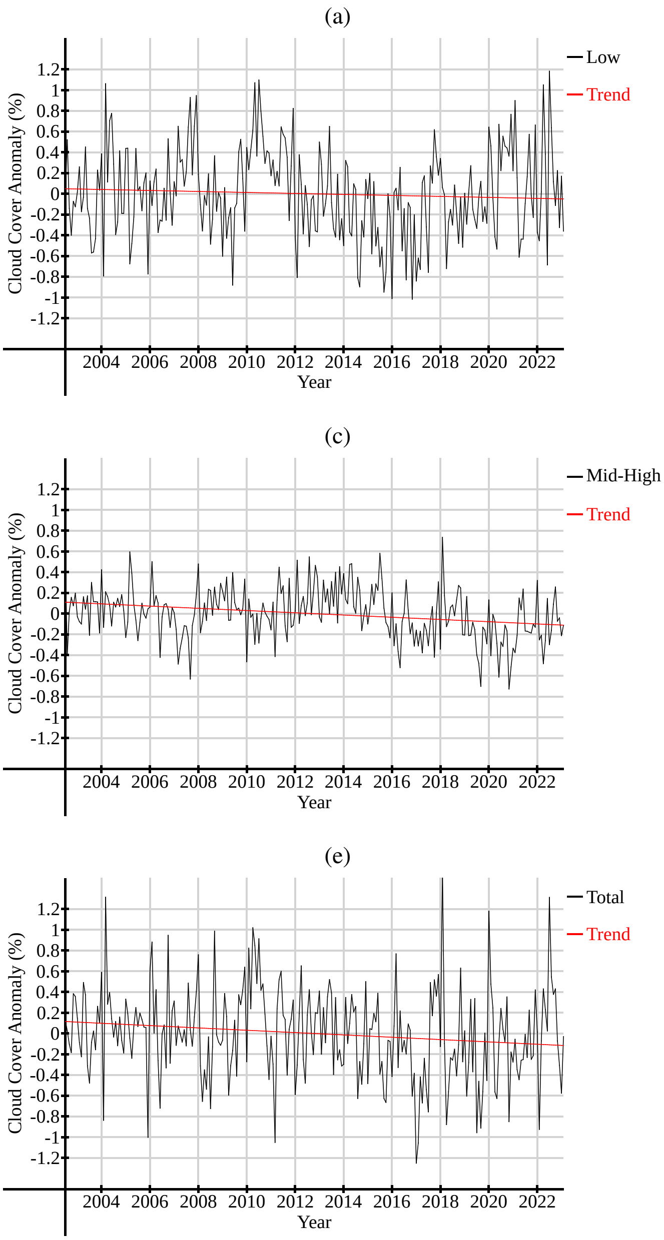

Figure A4. As Fig. A3 but for the day-time only cloud cover from CERES SSF.

A4 Comparison between cloud data

In this section, we compared all cloud datasets. A problem is that the datasets differ in the boundaries of the height levels: CLARA-A3 and ISCCP both distinguish 3 levels (low below 680 hPa, middle between 680 hPa and 440 hPa and high above 440 hPa), whereas CERES SSF distinguishes 4 levels (low below 700 hPa, mid-low between 700 hPa and 500 hPa, mid-high

https://doi.org/10.5194/egusphere-2025-418
Preprint. Discussion started: 24 February 2025

between 500 hPa and 300 hPa and high above 300 hPa). We used the height levels of CLARA-A3 and ISCCP and weighed CERES to their level (so for the generated low cloud data of CERES SSF, we use the CERES SSF low cloud data plus 0.1 times the mid-low cloud data and so on for the others).

In Fig. A5 we plotted the 3 datasets on the 3 different levels and the total cloud coverage for their entire period where they are deseasonalized over the overlapping period. We see that before 2000, the datasets again diverge, just as with the radiation data in Fig. 1 and 3. Also the cloud coverage of CERES and CLARA-A3 agree rather well on all heights and the ISCCP cloud data agrees less well, especially on the middle and high cloud coverage.

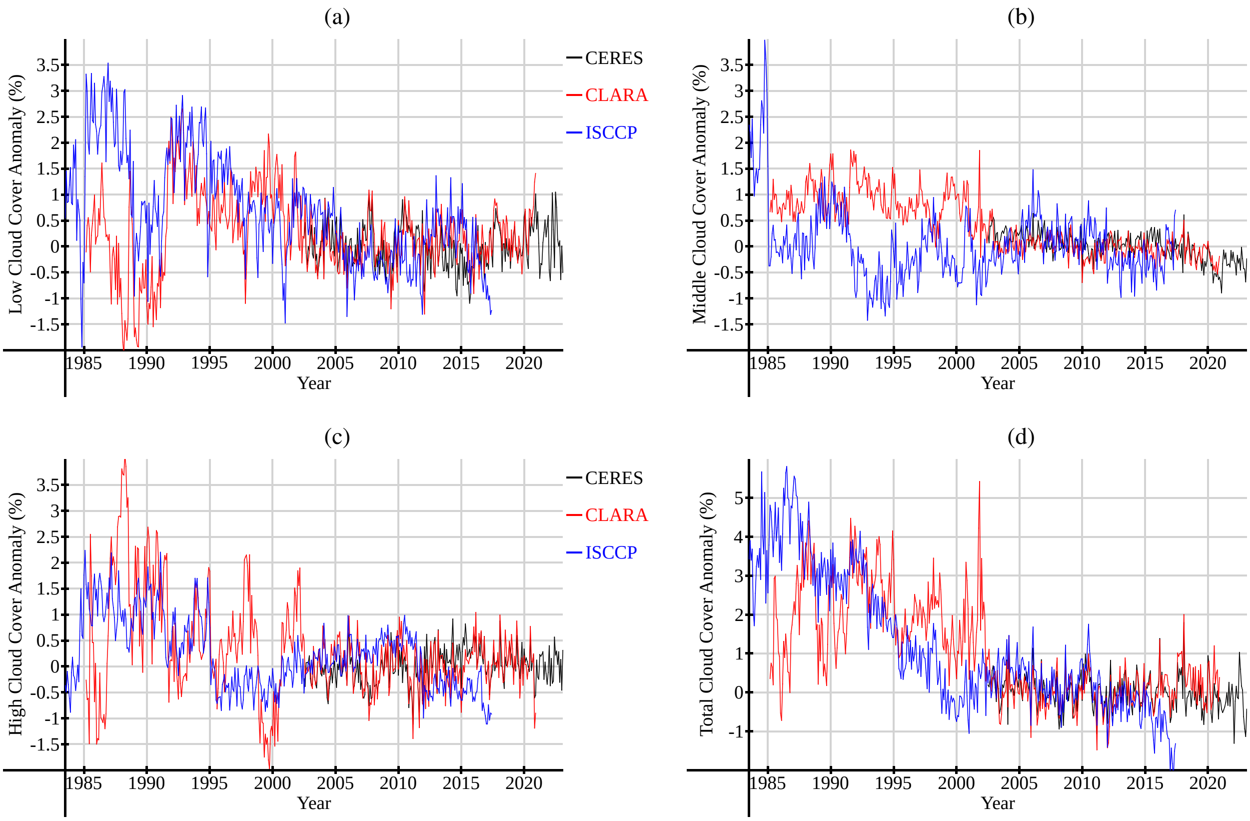

Figure A5. A comparison of the deseasonalized cloud coverage of CERES, CLARA-A3 and ISCCP on all three heights and on the total cloud cover: (a) shows the low cloud cover; (b) the middle cloud cover; (c) the high cloud cover; (d) the total cloud cover.

In Fig. A6, we zoomed in on the period from 2000 onward, as the period before is not homogeneous enough to tell us anything. CERES and CLARA-A3 agree well, especially on the high and middle cloud cover. For the low cloud cover, there seem to be some systematic difference which also present themselves in the total cloud cover. ISCCP on the other hand has systematic biases where it is too high before 2012 and too low afterwards for the high and middle cloud cover whereas it is the

https://doi.org/10.5194/egusphere-2025-418
Preprint. Discussion started: 24 February 2025

other way around for the low cloud cover. At the total cloud cover, it agrees a bit better until the last few years when the low cloud cover drops a lot compared to the other datasets.

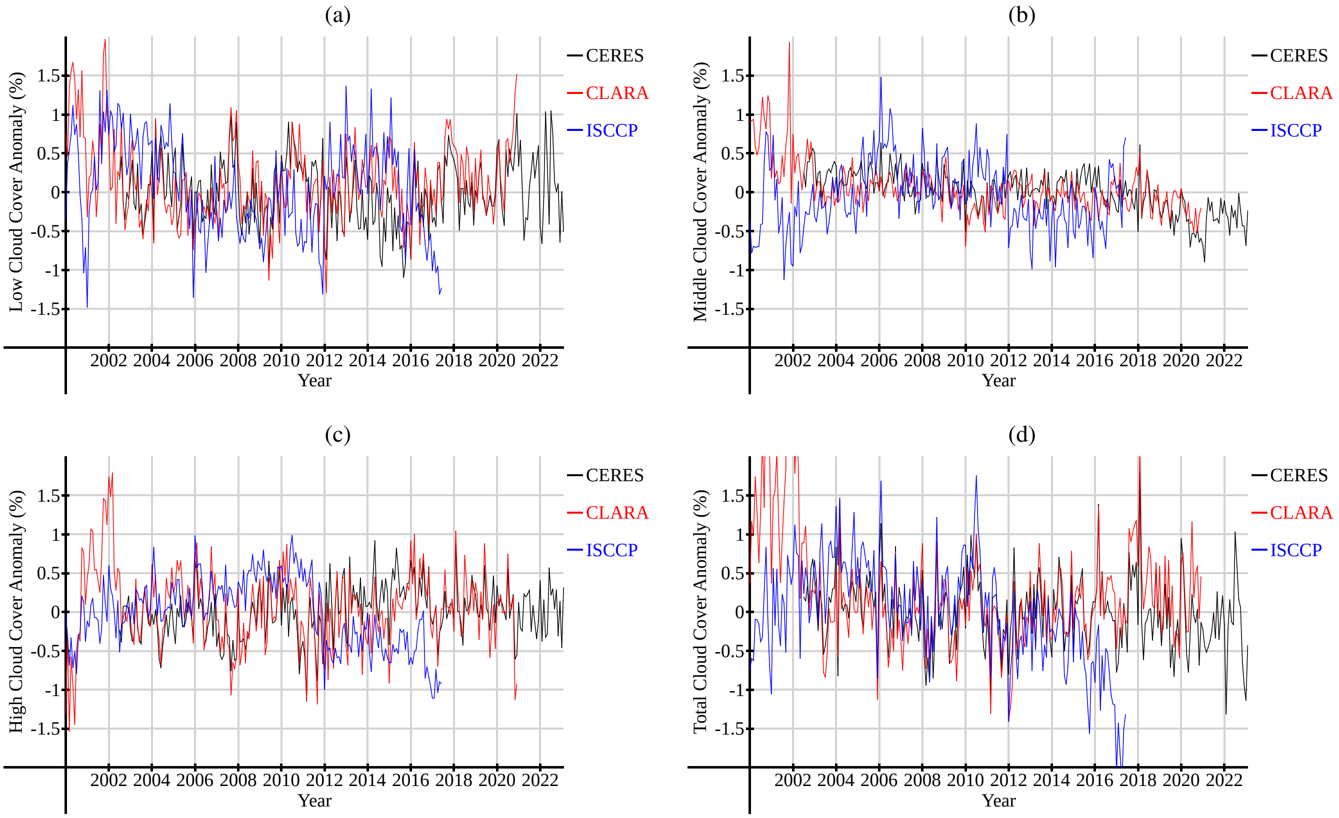

Figure A6. As Fig. A5 but for the period from 2000 onward only.

We saw that CLARA-A3 and CERES agree rather well whereas ISCCP disagrees more. As such we also examined the differences between CLARA-A3 and CERES at the three height levels below in Fig. A7 where we plotted the cloud cover from CLARA-A3 minus the cloud cover from CERES. For the low cloud cover, a fast increase in CLARA-A3 compared to CERES from July 2007 to September 2007 can be found. Next, a dip between say July 2009 and March 2012 followed by 2 jumps from March to April 2012 and from April to June 2013 are visible. Afterwards, there is a fast decrease from October to December 2015 and there do not seem to be clear differences afterwards. When using BEAST on these differences, it also finds break points in September 2007, June 2009, April 2012, June 2013 and November 2015 with probabilities 1, 1 0.75, 0.94 and 1. It also finds another break point in February 2019 with probability 0.81. The first jump in 2007 might be associated with the start of METOP-A in June 2007 from CLARA-A3, although this is uncertain. A possible cause for the jump in 2009 might be the start of the measurements of NOAA-19 in March 2009 or the transit to channel 3B in May 2009, but then it is

https://doi.org/10.5194/egusphere-2025-418
Preprint. Discussion started: 24 February 2025

strange that the break point is a few months later. In the same way, NOAA-16 stopped measuring in December 2011, which might have something to do with the break point in 2012, although it is again strange that the break point is a few months later. For the break point in 2013, we also see that METOP-B started measuring in January 2013, but then again the break point is a few months off. For the inhomogeneity at the end of 2015, there is no clear reason in the CLARA-A3 dataset and in CERES, the most likely cause would be the transit from MODIS C5 to MODIS C61 although that only happens in March 2016 which is again a few months off. For none of these possible break points, we thus have a clear idea what could have caused them and if they even are real inhomogeneities.

For the middle cloud cover, the datasets agree very well. There is only one real jump around April 2016 and a slight peak in the beginning from March 2007 to say May 2008. This is also supported when we use BEAST on the differences as it finds a break point in April 2016 with probability 0.99, a breakpoint in February 2007 with probability 0.84 and a break point in September 2008 with probability 0.74. The peak might very well be just noise and the jump in 2016 could be caused by the transit from MODIS C5 to MODIS C61 in CERES in March 2016.

For the high cloud cover, there is a dip from July 2007 to say October 2009 and a fast decrease from 2010 until 2015 and a jump from June 2015 to October 2015 after which the data series seem to agree. The fast decrease from 2010 to 2015 might also be a jump in January 2012 followed by a jump from August to October 2013. If we use BEAST, we get break points in July 2007, December 2009, January 2012 and September 2015 with probabilities 0.96, 0.98, 0.99 and 1. It is remarkable that the first 3 break points also seem to appear in the low cloud cover but then with opposite signs. Again for the jump in 2007, it might have been because METOP-A started measuring in June 2007. For the break point in 2009, this might be due to the start of NOAA-19 in March 2009, although it then remains strange that the break point only shows up later in 2009. The fact that NOAA-16 stopped measuring in December 2011 does coincide with the jump in January 2012. For the break point around September 2015, there is no clear reason in the CLARA-A3 dataset and in the CERES dataset, the only possibility seems to be the transit from MODIS C5 to MODIS C61 in March 2016, but that is rather late for this difference. For none of these break points, we can thus really be sure what caused them.

For the total cloud cover, there is a strange outlier visible at the start of 2012. Other than that, there again seems to be a small peak from October 2007 to April 2009 and a possible break points from June to September 2016. BEAST also finds this peak with break points in September 2007 and April 2009 with probabilities 0.962 and 0.827 but it does not really find a specific break points in 2016, most likely because it also resembles a gradual increase. For the peak this might again be caused by the start of METOP-A in June 2007 and NOAA-19 in March 2009, but it might also just be noise. For the possible inhomogeneity in 2016, this might be due to the transit of MODIS C5 to MODIS C61 in March 2016, but then it is again a bit late.

https://doi.org/10.5194/egusphere-2025-418
Preprint. Discussion started: 24 February 2025

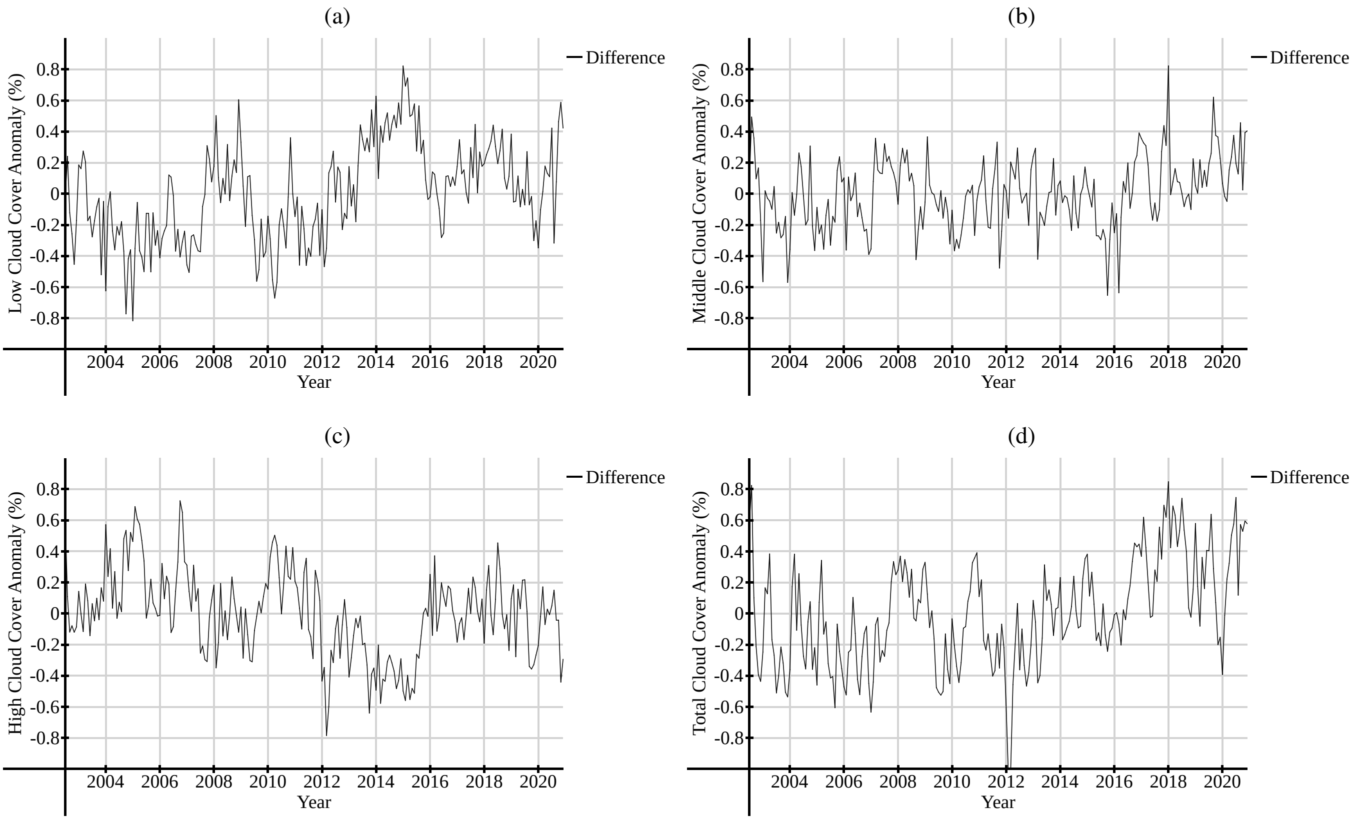

Figure A7. The cloud cover of CLARA-A3 minus the cloud cover of CERES over the period July 2002 until December 2020: (a) shows the difference in low cloud cover; (b) in middle cloud cover; (c) in high cloud cover; (d) in total cloud cover.

Author contributions. The research was initiated and conducted by Jippe Hoogeveen. Jan Fokke Meirink and Frank Selten supervised the project and helped to interpret the results.

Competing interests. The authors declare that they have no conflict of interest.

Acknowledgements. We would like to thank Gerard Barkema for supervising this thesis from Utrecht University.

https://doi.org/10.5194/egusphere-2025-418
Preprint. Discussion started: 24 February 2025

References

Allan, R. P., Willett, K. M., John, V. O., and Trent, T.: Global Changes in Water Vapor 1979–2020, Journal of Geophysical Research: Atmospheres, 127, e2022JD036 728, https://doi.org/https://doi.org/10.1029/2022JD036728, e2022JD036728 2022JD036728, 2022.

CERES: Data Quality Summary CERES EBAF 4.2, https://ceres.larc.nasa.gov/documents/DQ_summaries/CERES_EBAF_Ed4.2_DQS.pdf, 2024.

Chen, T., Rossow, W. B., and Zhang, Y.: Radiative Effects of Cloud-Type Variations, Journal of Climate, 13, 264 – 286, https://doi.org/10.1175/1520-0442(2000)013<0264:REOCTV>2.0.CO;2, 2000.

De Longueville, H., Clarisse, L., Whitburn, S., Franco, B., Bauduin, S., Clerbaux, C., Camy-Peyret, C., and Coheur, P.-F.: Identification of Short and Long-Lived Atmospheric Trace Gases From IASI Space Observations, Geophysical Research Letters, 48, e2020GL091 742, https://doi.org/https://doi.org/10.1029/2020GL091742, e2020GL091742 2020GL091742, 2021.

Dentener, F., Hall, B., and Smith, C.: IPCC, 2021: Annex III: Tables of historical and projected well-mixed greenhouse gas mixing ratios and effective radiative forcing of all climate forcers, Cambridge University Press, https://doi.org/10.1017/9781009157896.017, 2021.

Doelling, D. R., Loeb, N. G., Keyes, D. F., Nordeen, M. L., Morstad, D., Nguyen, C., Wielicki, B. A., Young, D. F., and Sun, M.: Geostationary Enhanced Temporal Interpolation for CERES Flux Products, Journal of Atmospheric and Oceanic Technology, 30, 1072 – 1090, https://doi.org/https://doi.org/10.1175/JTECH-D-12-00136.1, 2013.

Goessling, H. F., Rackow, T., and Jung, T.: Recent global temperature surge intensified by record-low planetary albedo, Science, 387, 68–73, https://doi.org/10.1126/science.adq7280, 2025.

Hersbach, H., Bell, B., Berrisford, P., Hirahara, S., Horányi, A., Muñoz-Sabater, J., Nicolas, J., Peubey, C., Radu, R., Schepers, D., Simmons, A., Soci, C., Abdalla, S., Abellan, X., Balsamo, G., Bechtold, P., Biavati, G., Bidlot, J., Bonavita, M., De Chiara, G., Dahlgren, P., Dee, D., Diamantakis, M., Dragani, R., Flemming, J., Forbes, R., Fuentes, M., Geer, A., Haimberger, L., Healy, S., Hogan, R. J., Hólm, E., Janisková, M., Keeley, S., Laloyaux, P., Lopez, P., Lupu, C., Radnoti, G., de Rosnay, P., Rozum, I., Vamborg, F., Villaume, S., and Thépaut, J.-N.: The ERA5 global reanalysis, Quarterly Journal of the Royal Meteorological Society, 146, 1999–2049, https://doi.org/https://doi.org/10.1002/qj.3803, 2020.

Karlsson, K.-G., Stengel, M., Meirink, J. F., Riihelä, A., Trentmann, J., Akkermans, T., Stein, D., Devasthale, A., Eliasson, S., Johansson, E., Håkansson, N., Solodovnik, I., Benas, N., Clerbaux, N., Selbach, N., Schröder, M., and Hollmann, R.: CLARA-A3: The third edition of the AVHRR-based CM SAF climate data record on clouds, radiation and surface albedo covering the period 1979 to 2023, Earth System Science Data, 15, 4901–4926, https://doi.org/10.5194/essd-15-4901-2023, 2023.

Kato, S., Rose, F. G., Rutan, D. A., Thorsen, T. J., Loeb, N. G., Doelling, D. R., Huang, X., Smith, W. L., Su, W., and Ham, S.-H.: Surface Irradiances of Edition 4.0 Clouds and the Earth's Radiant Energy System (CERES) Energy Balanced and Filled (EBAF) Data Product, Journal of Climate, 31, 4501 – 4527, https://doi.org/10.1175/JCLI-D-17-0523.1, 2018.

Kramer, R. J., He, H., Soden, B. J., Oreopoulos, L., Myhre, G., Forster, P. M., and Smith, C. J.: Observational evidence of increasing global radiative forcing, Geophysical Research Letters, p. e2020GL091585, https://doi.org/10.1029/2020GL091585, 2021.

Lee, H.-T., Gruber, A., Ellingson, R. G., and Laszlo, I.: Development of the HIRS Outgoing Longwave Radiation Climate Dataset, Journal of Atmospheric and Oceanic Technology, 24, 2029 – 2047, https://doi.org/10.1175/2007JTECHA989.1, 2007.

Loeb, N. G., Doelling, D. R., Wang, H., Su, W., Nguyen, C., Corbett, J. G., Liang, L., Mitrescu, C., Rose, F. G., and Kato, S.: Clouds and the Earth's Radiant Energy System (CERES) Energy Balanced and Filled (EBAF) Top-of-Atmosphere (TOA) Edition-4.0 Data Product, Journal of Climate, 31, 895 – 918, https://doi.org/https://doi.org/10.1175/JCLI-D-17-0208.1, 2018.

Loeb, N. G., Johnson, G. C., Thorsen, T. J., Lyman, J. M., Rose, F. G., and Kato, S.: Satellite and Ocean Data Reveal Marked Increase in Earth's Heating Rate, Geophysical Research Letters, 48, e2021GL093 047, https://doi.org/https://doi.org/10.1029/2021GL093047, e2021GL093047 2021GL093047, 2021.

Loeb, N. G., Doelling, D. R., Kato, S., Su, W., Mlynczak, P. E., and Wilkins, J. C.: Continuity in Top-of-Atmosphere Earth Radiation Budget Observations, Journal of Climate, 37, 6093 – 6108, https://doi.org/10.1175/JCLI-D-24-0180.1, 2024.

Masson-Delmotte, V., Zhai, P., Pirani, A., Connors, S., Péan, C., Berger, S., Caud, N., Chen, Y., Goldfarb, L., Gomis, M., Huang, M., Leitzell, K., Lonnoy, E., Matthews, J., Maycock, T., Waterfield, T., Yelekçi, O., Yu, R., and Zhou, B.: Climate Change 2021 – The Physical Science Basis: Working Group I Contribution to the Sixth Assessment Report of the Intergovernmental Panel on Climate Change, Cambridge University Press, https://doi.org/10.1017/9781009157896, 2023.

Olonscheck, D. and Rugenstein, M.: Coupled Climate Models Systematically Underestimate Radiation Response to Surface Warming, Geophysical Research Letters, 51, e2023GL106 909, https://doi.org/https://doi.org/10.1029/2023GL106909, e2023GL106909 2023GL106909, 2024.

Rossow, W. B., Knapp, K. R., and Young, A. H.: International Satellite Cloud Climatology Project: Extending the Record, Journal of Climate, 35, 141 – 158, https://doi.org/https://doi.org/10.1175/JCLI-D-21-0157.1, 2022.

Spencer R.W., C. J. . B.: W.D. UAH Version 6 global satellite temperature products: Methodology and results, Asia-Pacific J Atmos Sci, 53, 121–130, https://doi.org/https://doi.org/10.1007/s13143-017-0010-y, 2017.

Stengel, M., Stapelberg, S., Sus, O., Finkensieper, S., Würzler, B., Philipp, D., Hollmann, R., Poulsen, C., Christensen, M., and McGarragh, G.: Cloud_cci Advanced Very High Resolution Radiometer post meridiem (AVHRR-PM) dataset version 3: 35-year climatology of global cloud and radiation properties, Earth System Science Data, 12, 41–60, https://doi.org/10.5194/essd-12-41-2020, 2020.

Teixeira, J., Wilson, R. C., and Thrastarson, H. T.: Direct observational evidence from space of the effect of CO_2 increase on longwave spectral radiances: the unique role of high-spectral-resolution measurements, Atmospheric Chemistry and Physics, 24, 6375–6383, https://doi.org/10.5194/acp-24-6375-2024, 2024.

Whitburn, S., Clarisse, L., Bouillon, M., Safieddine, S., George, M., Dewitte, S., de Longeuville, H., Coheur, P.-F., and Clerbaux, C.: Trends in spectrally resolved outgoing longwave radiation from 10 years of satellite measurements, npj Climate and Atmospheric Science, 4, https://doi.org/10.1038/s41612-021-00205-7, 2021.

Young, A. H., Knapp, K. R., Inamdar, A., Hankins, W., and Rossow, W. B.: The International Satellite Cloud Climatology Project H-Series climate data record product, Earth System Science Data, 10, 583–593, https://doi.org/10.5194/essd-10-583-2018, 2018.

Zhao, K., Wulder, M. A., Hu, T., Bright, R., Wu, Q., Qin, H., Li, Y., Toman, E., Mallick, B., Zhang, X., and Brown, M.: Detecting change-point, trend, and seasonality in satellite time series data to track abrupt changes and nonlinear dynamics: A Bayesian ensemble algorithm, Remote Sensing of Environment, 232, 111 181, https://doi.org/https://doi.org/10.1016/j.rse.2019.04.034, 2019.